80558 MULTIRATE SIGNAL PROCESSING

Part V: Multirate Filter Banks

- During the last two decades, filter banks have found various applications in many areas, such as speech coding, scrambling, image compression, adaptive signal processing, and transmission of several signals through the same channel.
- The main idea of using filter banks is the ability of the system to separate in the frequency domain the signal under consideration into two or more signals or to compose two or more different signals into a single signal.
- When splitting the signal into two or more signals an analysis-synthesis system is used, as shown on the next page in the case where, for simplicity, only 4 sub-signals are used.
- In the analysis bank, the signal is split with the aid of four filters $H_k(z)$ for $k = 0,1,2,3$ into 4 bands of the same bandwidths and each sub-signal is decimated by a factor of 4.
- When splitting the signal into various frequency bands, the signal characteristics are different in each band and the various numbers of bits can be used for coding of the subsignals in the processing unit.
- The processing unit corresponds to storing the signal into the memory or transferring it through the channel.
- The main goal is to significantly reduce, with the aid of proper coding schemes, the number of bits representing the original signal for storing or transferring purposes.

Analysis-Synthesis Filter Bank

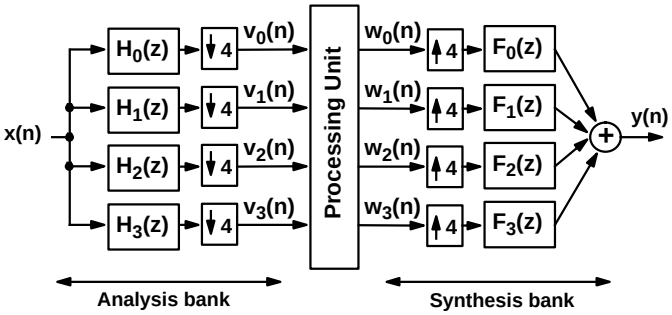

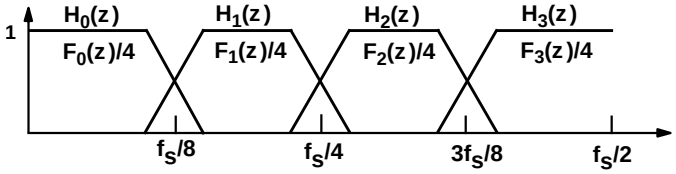

Analysis-Synthesis Filter Bank

- The role of the filters in the synthesis part is to reconstruct the original signal. In the case of the figure of the previous page, this is performed in two steps.
- First, the 4 sub-signals at the output of the processing unit are interpolated by a factor of 4 and filtered by 4 synthesis filters $F_k(z)$ for $k = 0,1,2,3$.
- Second, the outputs of these four filters are added.
- The target is to design the overall system in such a manner that, despite of a significantly reduced number of bits for storing and transferring purposes, the reconstructed signal is either the delayed version of the original signal or suffers from a negligible lost of the information carried by the subsignals.
- There are two types of coding techniques, namely, lossy and lossless codings. In the second case, it is possible to design the overall system such that the output signal is simply a delayed version of the input signal.
- The coding techniques are not at all considered in this course. In the sequel, we concentrate on the case where the processing unit does not cause any errors for the sub-signals.
- In the case of audio or speech signals, the goal is to design the overall system together with coding such that our ear is not able to notice the errors caused by reducing the number of bits used for storing or transferring purposes.

- In the case of images, our eyes serve as “referees”, that is, reduce the number of bits to represent the image to the limit it is satisfactory to our eyes. No more bits are needed!
- Depending on how many channels are used for the signal separation, there are two groups of filter banks: multichannel or M-channel filter banks ($M > 2$) and two-channel filter banks: $M = 2$.
- In the first group, the signal is separated into M different channels and in the second group into two channels.
- We start with the two-channel case.
- Using a tree-structure, two-channel filter banks can be used for building M-channel filter banks in the case where M is a power of two, as we shall see later on.
- A more effective way of building M-channel filter banks is to first design a prototype filter in a proper manner. The filters in the analysis and synthesis banks are then generated with the aid of this prototype filter by using a cosine modulation or a modified DFT.
- Two-channel filter banks are very useful in generating octave filter banks and discrete-time wavelet banks.
- In these cases, the overall signal is first split into two bands. After that, the lowpass filtered signal is split into two bands and so on.
- In the case of discrete-time wavelet banks, the frequency selectivity of the filters in the octave analysis-synthesis filter banks is not so important due to their different applications. There are other properties that are more important, as will be pointed out later on.

- When two or more different signals are composed into a single signal, then a synthesis-analysis system is used, as shown on the next page for the case of 4 signals.
- This is also called a transmultiplexer.
- In this system, all the 4 signals are interpolated by a factor of 4 and filtered by 4 synthesis filters $F_k(z)$ for $k = 0,1,2,3$.
- Then, the outputs are added to give a single signal with sampling rate being 4 times that of the input signals.
- The next step is to transfer the signal through a channel.
- Finally, in the analysis bank the original signals are reconstructed with the aid of 4 analysis filters $H_k(z)$ for $k = 0,1,2,3$.
- These signals have the original sampling rates due to the decimation be a factor of 4.
- In the sequel, it is assumed that the channel is ideal. If not, some compensation filters are needed in the synthesis bank.
- If the output signal in the analysis-synthesis system (without coding) is just a delayed version of the input signal, then for the corresponding transmultiplexer the output signals (in the case of the ideal channel) are delayed versions of the inputs.
- Therefore, the design of a transmultiplexer can be converted to the design of an analysis-synthesis filter bank.
- In the sequel, we concentrate only on designing analysis-synthesis banks. If you are interested in transmultiplexers, please read the textbook written by Prof. Fliege (see Page 7).

Synthesis- Analysis Filter Bank, Transmultiplexer

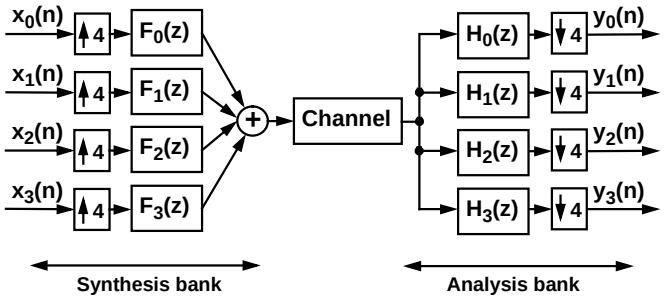

Material about Filter and Wavelet Banks

- H. S. Malvar, *Signal processing with Lapped Transforms*. Norwood: Artec House, 1992.
- P. P. Vaidyanathan, *Multirate Systems and Filter Banks*. Englewood Cliffs, N.J.: Prentice Hall, 1993.
- N. J. Fliege, *Multirate Digital Signal Processing*. Chicester: John Wiley and Sons, 1994.
- M. Vettereli and J. Kovacevic, *Wavelets and Subband Coding*. Englewood Cliffs, N.J.: Prentice Hall, 1995.
- R. Bregović and T. Saramäki, "Two-channel FIR filter banks – A tutorial review and new results," in *Proc. Second Int. Workshop on Transforms and Filter Banks*, Brandenburg, Germany, March 1999.

Multirate Filter Banks to be Considered

- This part of the course is divided into the following subparts:

I. Part V.A: Two-Channel FIR Filter Banks

II. Part V.B: Two-Channel IIR Filter Banks

III. Part V.C: Tree-Structured Filter Banks

IV. Part V.E: Discrete-Time Wavelet banks

V. Part V.D: Octave Filter Banks

VI. Part. V.F: Cosine-Modulated Filter Banks

Part V.A: Two-Channel FIR Filter Banks

- A two-channel filter bank consists of the analysis and the synthesis banks as well as the processing unit between these two banks, as shown below.

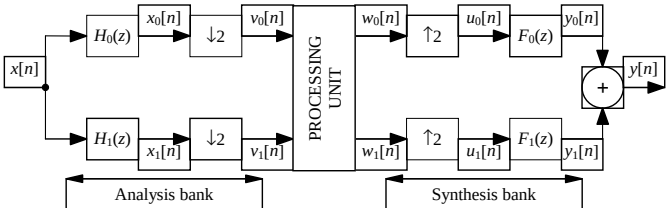

Figure 1. Two-channel filter bank

1. Analysis bank

- The analysis bank splits the input signal $x[n]$ into lowpass and highpass filtered channel signals $x_0[n]$ and $x_1[n]$ using a lowpass–highpass filter pair with transfer functions $H_0(z)$ and $H_1(z)$.
- The z-transforms of these signals are expressible in terms of $X(z)$, the z-transform of $x[n]$, as

$$X_k(z) = H_k(z)X(z) \quad \text{for} \quad k = 0,1. \tag{1}$$

- Then, the signals in both channels are down-sampled by a factor of two by picking up every second sample, resulting into two sub-band signal components $v_0[n]$ and $v_1[n]$.

- The z-transforms of these components are given by

$$V_k(z) = \frac{1}{2}\left[X_k\left(z^{1/2}\right) + X_k\left(-z^{1/2}\right)\right] \tag{2}$$

$$= \frac{1}{2}\left[H_k\left(z^{1/2}\right)X\left(z^{1/2}\right) + H_k\left(-z^{1/2}\right)X\left(-z^{1/2}\right)\right] \text{ for } k = 0,1.$$

- If the input sampling rate is F_s, then the sampling rates of $v_0[n]$ and $v_1[n]$ are $F_s/2$.
- The corresponding relations between the Fourier transforms are obtained by using the substitution $z = e^{j2\pi f/F_s}$ in Eq. (1) and $z = e^{j2\pi f/(F_s/2)}$ in Eq. (2) as well as the identity $-1 = e^{j\pi}$.
- This yields for $k = 0,1$

$$X_k\left(e^{j2\pi f/F_s}\right) = H_k\left(e^{j2\pi f/F_s}\right)X\left(e^{j2\pi f/F_s}\right) \tag{3a}$$

and

$$V_k\left(e^{j2\pi f/(F_s/2)}\right) = \frac{1}{2}\left[X_k(e^{j2\pi f/F_s}) + X_k\left(e^{j2\pi(f+F_s/2)/F_s}\right)\right]. \tag{3b}$$

- $H_0(z)$ and $H_1(z)$ usually have the same transition band region with the band edges located around $f = F_s/4$ at $f = (1-\rho_1)F_s/4$ and $f = (1+\rho_2)F_s/4$ with $\rho_1 > 0$ and $\rho_2 > 0$, as shown in Figure 2(b).
- In order to give a pictorial viewpoint of what is happening in the frequency domain, Figure 2(a) shows the Fourier transforms of an input signal $x[n]$, whereas Figure 3 shows those of the signals $x_0[n]$, $x_1[n]$, $v_0[n]$, and $v_1[n]$.

Figure 2. (a) Fourier transform of an input signal $x[n]$. (b) Amplitude responses for $H_0(z)$ and $H_1(z)$. (c) Amplitude responses for $F_0(z)$ and $F_1(z)$.

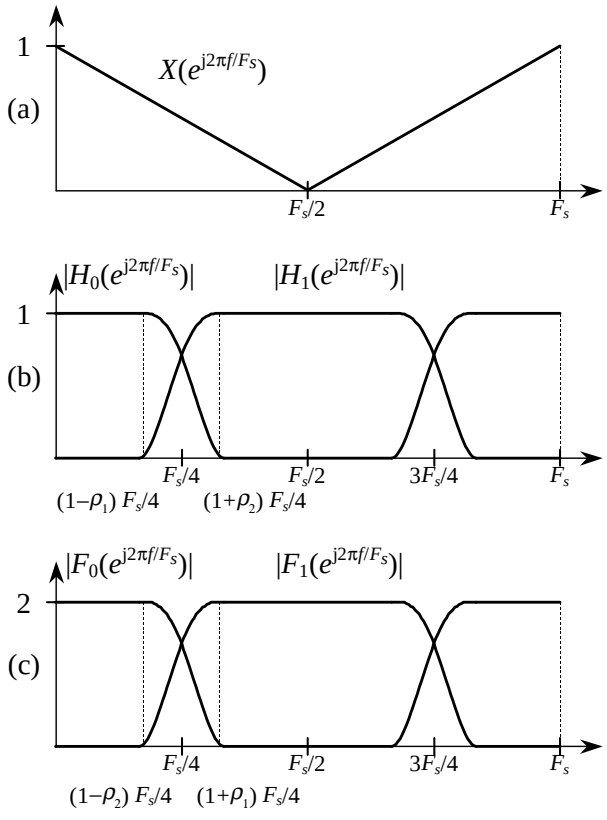

Figure 3. Magnitudes of the Fourier transforms of the signals in the two-channel filter bank of Figure 1.

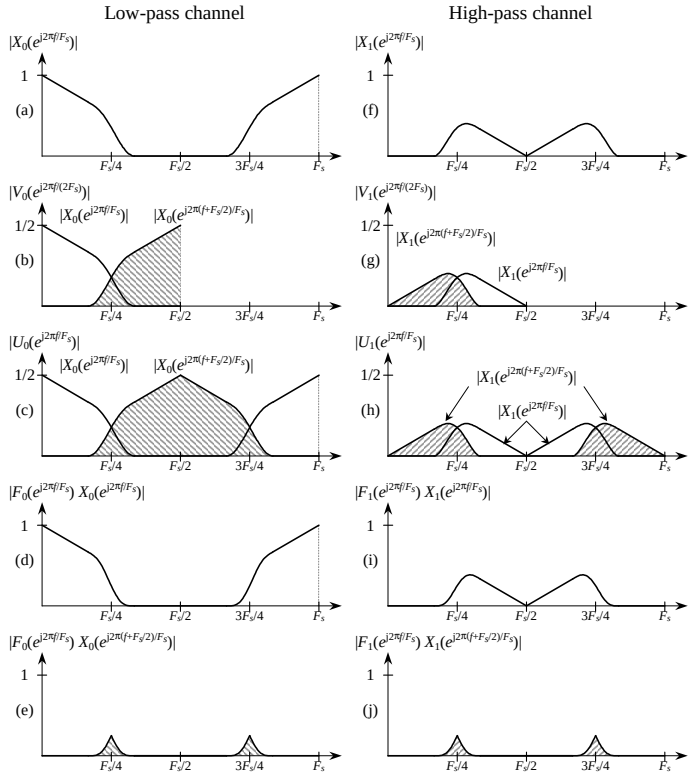

- As shown in Figures 3(b) and 3(g), $V_k(e^{j2\pi f/(F_s/2)})$ for $k = 0, 1$ contains in the baseband $[0, F_s/4]$ two overlapping frequency components $X_k(e^{j2\pi f/F_s})$ and $X_k(e^{j2\pi(f+F_s/2)/F_s})$.
- This overlapping can, however, be totally or partially eliminated in the overall system of Figure 1 by properly relating the transfer functions $H_0(z)$, $H_1(z)$, $F_0(z)$, and $F_1(z)$ to each other, as will be seen later on.

2. Processing Unit

- In the processing unit, the signals $v_0[n]$ and $v_1[n]$ are compressed and coded suitably for either transmission or storage purposes.
- Before using the synthesis part, both channel signals are decoded.
- The resulting signals denoted by $w_0[n]$ and $w_1[n]$ in Figure 1 may differ from the original signals $v_0[n]$ and $v_1[n]$ due to possible distortions caused by coding and quantization errors as well as channel impairments.
- In the sequel, it is supposed, for simplicity, that there are no coding, quantization, or channel degradations, that is, $w_0[n] \equiv v_0[n]$ and $w_1[n] \equiv v_1[n]$.

3. Synthesis Bank

- The role of the synthesis bank is to approximately reconstruct in three steps the delayed version of the original signal from the signal components $w_0[n]$ and $w_1[n]$.
- First, these signals are up-sampled by a factor of two by inserting zero-valued samples between the existing samples yielding two components $u_0[n]$ and $u_1[n]$ (see Figure 1).
- In the $w_0[n] \equiv v_0[n]$ and $w_1[n] \equiv v_1[n]$ case, the z- and Fourier transforms of these signals are expressible as

$$U_k(z) = V_k(z^2) = \frac{1}{2}[X_k(z) + X_k(-z)] \quad \text{for} \quad k = 0,1 \tag{4a}$$

and

$$\begin{aligned} U_k(e^{j2\pi f/F_s}) &= V_k(e^{j2\pi f/F_s}) \\ &= \frac{1}{2}\left[X_k(e^{j2\pi f/F_s}) + X_k(e^{j2\pi(f+F_s/2)/F_s})\right] \quad \text{for} \quad k = 0,1. \end{aligned} \tag{4b}$$

- Simultaneously, the sampling rate is increased from $F_s/2$ to F_s as well as the baseband from $[0, F_s/4]$ to $[0, F_s/2]$.
- Therefore, $u_0[n]$ and $u_1[n]$ contain in their basebands $[0, F_s/2]$, in addition to the frequency components of $v_0[n]$ and $v_1[n]$ in their basebands $[0, F_s/4]$, the components in $[F_s/4, F_s/2]$, as illustrated in Figures 3(c) and 3(h).
- In the time domain, the relations between the $u_k[n]$'s and $x_k[n]$'s are given by

$$u_k[n] = x_k[n]/2 + (-1)^n x_k[n]/2 \quad \text{for} \quad k = 0,1. \tag{5}$$

- Here, $x_k[n]$ is the desired unaliased signal component with the z-transform being $X_k(z)$, whereas $(-1)^n x_k[n]$ is the unwanted aliased signal component with the z-transform being $X_k(-z)$.
- The second step involves processing $u_0[n]$ and $u_1[n]$ by a lowpass–highpass filter pair with transfer functions $F_0(z)$ and $F_1(z)$
- The third step is to add the filtered signals, denoted by $y_0[n]$ and $y_1[n]$ in Figure 1, to yield the overall output $y[n]$. The z-transform of $y[n]$ is thus given by

$$Y(z) = Y_1(z) + Y_2(z) \tag{6a}$$

where for $k = 0, 1$

$$Y_k(z) = F_k(z)V_k(z^2) = \frac{1}{2}[F_k(z)X_k(z) + F_k(z)X_k(-z)] \tag{6b}$$

- The corresponding Fourier transform is expressible as

$$Y(e^{j2\pi f/F_s}) = Y_0(e^{j2\pi f/F_s}) + Y_1(e^{j2\pi f/F_s}) \tag{7a}$$

where for $k = 0, 1$

$$\begin{aligned} Y_k(e^{j2\pi f/F_s}) &= \frac{1}{2}F_k(e^{j2\pi f/F_s})X_k(e^{j2\pi f/F_s}) \\ &+ \frac{1}{2}F_k(e^{j2\pi f/F_s})X_k(e^{j2\pi(f+F_s/2)/F_s}) \ . \end{aligned} \tag{7b}$$

- The role of the synthesis filters with transfer functions $F_0(z)$ and $F_1(z)$ is twofold.

- First, it is desired that $Y(e^{j2\pi f/F_s})$ does not contain the terms $X_0\left(e^{j2\pi(f+F_s/2)/F_s}\right)$ and $X_1\left(e^{j2\pi(f+F_s/2)/F_s}\right)$.
- This is achieved if [see Figures 3(e) and 3(j)]

$$F_0\left(e^{j2\pi f/F_s}\right)X_0\left(e^{j2\pi(f+F_s/2)/F_s}\right)\approx -F_1\left(e^{j2\pi f/F_s}\right)X_1\left(e^{j2\pi(f+F_s/2)/F_s}\right).$$

- Second, $y[n]$ is desired to be approximately a delayed version of $x[n]$, that is, $y[n] \approx x[n-K]$.
- This is achieved if [see Figures 3(d) and 3(i)]

$$F_0\left(e^{j2\pi f/F_s}\right)X_0\left(e^{j2\pi f/F_s}\right)+F_1\left(e^{j2\pi f/F_s}\right)X_1\left(e^{j2\pi f/F_s}\right)\approx e^{-j2\pi fK/F_s}X\left(e^{j2\pi f/F_s}\right).$$

- In order to satisfy these requirements, the first condition is that $F_0(z)$ and $F_1(z)$ generate a lowpass–highpass filter pair having the same transition band region with the band edges at $f=(1-\rho_2)F_s/4$ and $f=(1+\rho_1)F_s/4$, as shown in Figure 2(c).
- As shown in Figure 2(c), the main difference is that now, because of interpolation, the amplitude responses should approximate two in the passbands. Furthermore, the edges have changed due to the fact $F_0(z)$ [$F_1(z)$] is related to $H_1(z)$ [$H_0(z)$] in the manner to be seen later on.
- The exact simultaneous conditions for $H_0(z)$, $H_1(z)$, $F_0(z)$, and $F_1(z)$ to satisfy the above-mentioned two conditions will be given next in the case where the filters are finite-impulse response (FIR) filters.

Alias-Free Two-Channel FIR Filter Banks

- Combining Eqs. (1) and (6) yields the following relation between the z-transforms of the input and output signals of Figure 1:

$$Y(z)=T(z)X(z)+A(z)X(-z) \tag{8a}$$

where

$$T(z)=\frac{1}{2}[H_0(z)F_0(z)+H_1(z)F_1(z)] \tag{8b}$$

and

$$A(z)=\frac{1}{2}[H_0(-z)F_0(z)+H_1(-z)F_1(z)]. \tag{8c}$$

- In the above equation, $X(-z)$ is the z-transform the undesired aliased signal being related to the original input signal $x[n]$ in the time domain through $(-1)^n x[n]$.
- In the sequel, we concentrate on designing filter banks where this term is absent, that is, $A(z) \equiv 0$. The most straightforward way of achieved this is to select $F_0(z)$ and $F_1(z)$ as follows:

$$F_0(z)=2H_1(-z) \tag{9a}$$

and

$$F_1(z)=-2H_0(-z). \tag{9b}$$

- In this case, the input-output relation of Equation (8a) takes the following simplified form:

$$Y(z)=T(z)X(z) \tag{10a}$$

where

$$T(z)=H_0(z)H_1(-z)-H_0(-z)H_1(z) \tag{10b}$$

- The restrictions of Eq. (9) convert the overall problem to designing the analysis filter pair.
- In the sequel, we concentrate on the banks where both $H_0(z)$ and $H_1(z)$ are transfer functions of FIR filters, that is, they are of the following forms:

$$H_0(z)=\sum_{n=0}^{N_0}h_0[n]z^{-n} \tag{11a}$$

and

$$H_1(z)=\sum_{n=0}^{N_1}h_1[n]z^{-n}. \tag{11b}$$

- Correspondingly, due to Eq. (9), $F_0(z)$ and $F_1(z)$ are of the forms:

$$F_0(z)=\sum_{n=0}^{N_1}f_0[n]z^{-n} \tag{12a}$$

and

$$F_1(z)=\sum_{n=0}^{N_0}f_1[n]z^{-n}, \tag{12b}$$

where

$$f_0[n]=\begin{cases}2h_1[n] & \text{for } n \text{ even}\\ -2h_1[n] & \text{for } n \text{ odd}\end{cases} \tag{12c}$$

and

$$f_1[n]=\begin{cases}-2h_0[n] & \text{for } n \text{ even}\\ 2h_0[n] & \text{for } n \text{ odd.}\end{cases} \tag{12d}$$

Perfect-Reconstruction (PR) Two-Channel FIR Filter Banks

The necessary conditions for the Perfect-reconstruction (PR) property are given in the following theorem:

Theorem for the PR property: Consider the two-channel filter bank shown in Figure 1 with $w_0[n] \equiv v_0[n]$ and $w_1[n] \equiv v_1[n]$ and let $H_0(z)$, $H_1(z)$, $F_0(z)$ and $F_1(z)$ be given by Eqs. (11) and (12). Then, $y[n] = x[n-K]$ with K odd if the impulse-response coefficients of

$$E(z) = H_0(z)H_1(-z) = \sum_{n=0}^{N_0+N_1} e[n]z^{-n} \tag{13}$$

satisfy

$$e[n] = \begin{cases} 1/2 & \text{for } n = K \\ 0 & \text{for } n \text{ is odd and } n \neq K. \end{cases} \tag{14}$$

- In order to proof this theorem, Equation (10b) is rewritten as

$$\begin{aligned} T(z) &= \sum_{n=0}^{N_0+N_1} t[n]z^{-n} = E(z) + [-E(-z)] = \\ &= \sum_{n=0}^{N_0+N_1} (e[n] + \hat{e}[n])z^{-n} \end{aligned} \tag{15a}$$

where

$$\hat{e}[n] = \begin{cases} -e[n] & \text{for } n \text{ even} \\ e[n] & \text{for } n \text{ odd.} \end{cases} \tag{15b}$$

- From Eqs. (14) and (15), it then follows that the impulse-response coefficients of $T(z)$ satisfy

$$t[n] = e[n] + \hat{e}[n] = \begin{cases} 1 & \text{for } n = K \\ 0 & \text{for } n \neq K, \end{cases} \tag{16}$$

yielding

$$T(z) = z^{-K}. \tag{17}$$

- There are two basic alternatives to achieve the PR property, namely, $K = (N_0+N_1)/2$ and $K < (N_0+N_1)/2$, as illustrated in Figures 4(a) and 4(b), respectively.
- In the first case, $E(z)$ is an FIR filter transfer function with a symmetric impulse response and the impulse-response value occurring at the odd central point $n = K$ is equal to 1/2, whereas the other values occurring at odd values of n are zero. Hence, $E(z)$ is a transfer function of an FIR half-band filter.
- In the second case, the impulse-response values at odd values of n are also zero except for one odd value of $n = K$, where the impulse response takes on the value of 1/2.
- The $K = (N_0+N_1)/2$ case is attractive when the overall delay of K samples is tolerable, whereas the $K < (N_0+N_1)/2$ case is used for reducing the delay caused by the filter bank to the overall signal.

Figure 4. Impulse responses for $E(z)$, $E(-z)$, and $T(z)$ for PR filter banks. (a) $K = (N_0+N_1)/2$. (b) $K < (N_0+N_1)/2$.

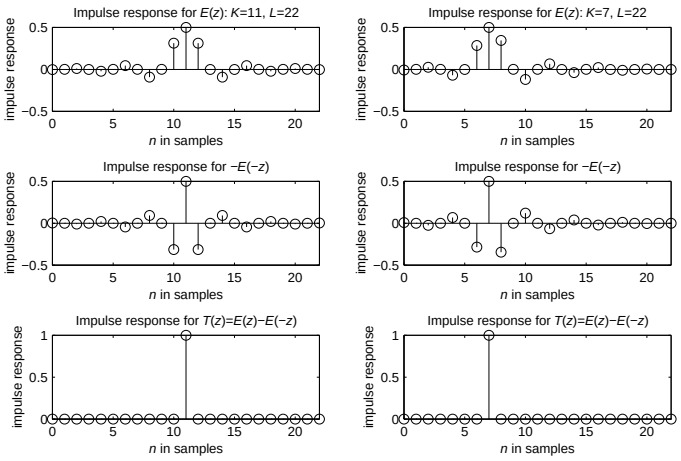

Nearly Perfect-Reconstruction (NPR) Two-Channel FIR Filter Banks

- The frequency response between the input and output signal for the alias-free banks is expressible as

$$T(e^{j\omega}) = e^{-jK\omega}\hat{T}(e^{j\omega}), \tag{18a}$$

where

$$\hat{T}(e^{j\omega}) = \sum_{n=0}^{N_0+N_1} t[n]e^{-j(n-K)\omega}. \tag{18b}$$

- Here, $t[n] = e[n] + \hat{e}[n]$ with the $e[n]$'s $n = 0, 1, \cdots, N_0 + N_1$ being the impulse-response coefficients of $H_0(z)H_1(-z)$ and the $\hat{e}[n]$'s being related to the $e[n]$'s according to Eq. (15b).
- In the PR case, $\hat{T}(e^{j\omega}) \equiv 1$ so that there is no amplitude or phase distortion. This is due to the fact that $t[n]$ is nonzero only at $n = K$ achieving the value of unity.
- In the nearly perfect-reconstruction (NPR) case, the impulse-response values $t[n]$ differ slightly from zero for $n \neq K$ and slightly from 1 for $n = K$ so that there exists some amplitude distortion and phase distortion.
- As will be seen later on, the phase distortion takes place only for $K < (N_0+N_1)/2$. For $K = (N_0+N_1)/2$, $t[2K-n] = t[n]$ for $n = 0, 1, \cdots, K-1$, making $\hat{T}(e^{j\omega})$ a real-valued function.
- As a matter of fact, $T(z)$ as given by Equation (15a) becomes in this case a transfer function of a linear-phase filter of or-

der $2K$ and $\hat{T}(e^{j\omega})$ is the zero-phase frequency response of this filter.

- In the above, the substitution $z = e^{j\omega}$, instead of $z = e^{j2\pi f / F_s}$, is used for simplicity to express the frequency response in terms of the angular frequency $\omega = 2\pi f / F_s$.
- In the sequel, in order to simplify the equations, the same substitution will be used.

Primary Transfer Functions under Consideration

- In order to simply the synthesis of two-channel FIR filter banks, we concentrate on designing the following transfer functions:

$$G_0(z) = \sum_{n=0}^{N_0} g_0[n] z^{-n} \equiv H_0(z) = \sum_{n=0}^{N_0} h_0[n] z^{-n} \qquad (19a)$$

and

$$G_1(z) = \sum_{n=0}^{N_1} g_1[n] z^{-n} \equiv H_1(-z) = \sum_{n=0}^{N_1} (-1)^n h_1[n] z^{-n}. \qquad (19b)$$

- In the above, $G_0(z)$ and $H_0(z)$ are identical with $g_0[n] \equiv h_0[n]$ for $n = 0, 1, \cdots, N_0$.
- For the filters with transfer functions $G_1(z)$ and $H_1(z)$, the frequency responses, the amplitude responses, and the impulse-response coefficients are related through $G_1(e^{j\omega}) = H_1(e^{j(\omega+\pi)})$ or $H_1(e^{j\omega}) = G_1(e^{j(\omega+\pi)})$; $|G_1(e^{j\omega})| = |H_1(e^{j(\pi-\omega)})|$ or $|H_1(e^{j\omega})| = |G_1(e^{j(\pi-\omega)})|$; and $g_1[n] = (-1)^n h_1[n]$ or $h_1[n] = (-1)^n g_1[n]$ for $n = 0, 1, \cdots, N_1$, respectively.
- Based on the these relations, $G_1(z)$ is a transfer function of a lowpass filter with the amplitude response obtained from the corresponding highpass filter with transfer function $H_1(z)$ reversing the frequency response using the substitution $\pi - \omega \rightarrow \omega$.

- Figure 5 exemplifies the above relations in addition to showing the constraints for $G_0(z)$ and $G_1(z)$ to be stated in the general optimization problem to be considered later.
- The basic reason for taking the transfer functions $G_0(z)$ and $G_1(z)$ as preliminary ones lies in the fact that both of them are lowpass transfer functions, making the synthesis of two-channel FIR filter banks more straightforward, as will be seen later.
- Once $G_0(z)$ and $G_1(z)$ have been designed, then the corresponding impulse-response coefficients of $H_0(z)$ and $H_1(z)$ are given by $h_0[n] \equiv g_0[n]$ for $n = 0, 1, \cdots, N_0$ and $h_1[n] = (-1)^n g_1[n]$ for $n = 0, 1, \cdots, N_1$, respectively.
- In terms of $G_0(z)$ and $G_1(z)$, the overall transfer function is given by

$$T(z) = G_0(z)G_1(z) - G_0(-z)G_1(-z). \qquad (20)$$

- The perfect reconstruction implies now that the impulse-response coefficients of

$$E(z) = G_0(z)G_1(z) = \sum_{n=0}^{N_0+N_1} e[n] z^{-n} \qquad (21a)$$

satisfy for an odd integer K

$$e[n] = \begin{cases} 1/2 & \text{for } n = K \\ 0 & \text{for } n \text{ is odd and } n \neq K. \end{cases} \qquad (21b)$$

- Furthermore N_0+N_1 should be two times an odd integer.

Figure 5. Specifications for $G_0(z)$ and $G_1(z)$ as well as the relations between $H_0(z)$ and $G_0(z)$ and $H_1(z)$ and $G_1(z)$.

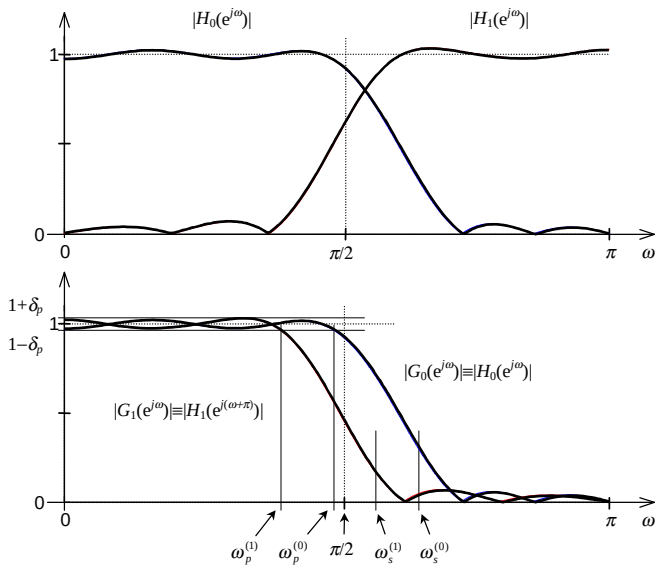

Two-Channel FIR Filter Banks Under Consideration

- We concentrate on the following alias-free two-channel FIR filter banks:

1. NPR quadrature mirror filter banks: $G_1(z) = G_0(z)$:
   a) $G_0(z)$ is a linear-phase FIR filter and the overall delay satisfies $K = N_0$.
   b) $G_0(z)$ is a nonlinear-phase FIR filter and the overall delay satisfies $K < N_0$.
2. PR orthogonal filter banks: $G_1(z) = z^{-N_0} G_0(z^{-1})$ and $K = N_0$.
3. PR biorthogonal filter banks:
   a) $G_0(z)$ and $G_1(z)$ are different linear-phase FIR filters and $K = (N_0+N_1)/2$.
   b) $G_0(z)$ and $G_1(z)$ are different nonlinear-phase FIR filters and $K < (N_0+N_1)/2$.
4. Generalized NPR filter banks:
   a) $G_0(z)$ and $G_1(z)$ are different linear-phase FIR filters and $K = (N_0+N_1)/2$.
   b) $G_0(z)$ and $G_1(z)$ are different nonlinear-phase FIR filters and $K \le (N_0+N_1)/2$.

General Optimization Problem:

Given the class of two-channel filter banks, N_0, N_1, $\rho_p^{(k)}$ and $\rho_s^{(k)}$ for $k = 0$, 1, δ_a, and δ_p as well as K, find the adjustable coefficients of $G_0(z)$ and $G_1(z)$, as given by Equations (19a) and (19b), to minimize

$$\varepsilon = \max(\varepsilon_0, \varepsilon_1), \tag{22a}$$

where

$$\varepsilon_k = \int_{\omega_s^{(k)}}^{\pi} \left| G_k\left(e^{j\omega}\right) \right|^2 d\omega \quad \text{for} \quad k = 0,1 \tag{22b}$$

subject to

$$\max_{\omega \in [0,\pi]} \left| T\left(e^{j\omega}\right) - e^{-jK\omega} \right| \le \delta_a, \tag{22c}$$

$$\max_{\omega \in \left[0, \omega_p^{(k)}\right]} \left| \left| G_k\left(e^{j\omega}\right) \right| - 1 \right| \le \delta_p \quad \text{for} \quad k = 0, 1, \tag{22d}$$

and

$$\max_{\omega \in \left(\omega_p^{(k)}, \omega_s^{(k)}\right)} \left| G_k\left(e^{j\omega}\right) \right| - 1 \le \delta_p \quad \text{for} \quad k = 0,1. \tag{22e}$$

- Here, $\omega_s^{(k)} = (1+\rho_s^{(k)})\pi/2$ and $\omega_p^{(k)} = (1-\rho_p^{(k)})\pi/2$ for $k = 0,1$ and $T\left(e^{j\omega}\right) = G_0\left(e^{j\omega}\right)G_1\left(e^{j\omega}\right) - G_0\left(e^{j(\omega+\pi)}\right)G_1\left(e^{j(\omega+\pi)}\right)$ is the frequency response for the overall system of Figure 1.

Comment on the Stated Problem

- In the stated problem, the passband and stopband regions of $G_k(z)$ for $k = 0$, 1 are $[0, \omega_p^{(k)}]$ and $[\omega_s^{(k)}, \pi]$. The edges have been defined in terms of the positive quantities $\rho_p^{(k)}$ and $\rho_s^{(k)}$ for $k = 0$, 1 to make the passband edges [stopband edges] less than [larger than] $\pi/2$.
- The main objective is to minimize the maximum of the stopband energies of $G_0(z)$ and $G_1(z)$ subject to some constraints, as illustrated in Figure 5.
- First, the maximum of the absolute value of the deviation between the overall frequency response and a constant delay of K samples has to stay in the overall frequency range within the given limits $\pm\delta_a$.
- For the PR filter banks, this deviation is zero.
- Second, amplitude responses of both $G_0(z)$ and $G_1(z)$ have to stay in the passband within the given limits $1\pm\delta_p$.
- Third, the maximum allowable value for these amplitude responses in the transition bands is $1+\delta_p$.
- As will be seen later, some of the constraints are automatically satisfied for some of the above-mentioned types of two-channel filter banks.

How to Proceed for the Rest of the Description of Two-Channel FIR Filter Banks

- A very comprehensive review on the existing and new proposed synthesis techniques can be found in:
- R. Bregović and T. Saramäki, "Two-channel FIR filter banks – A tutorial review and new results," in *Proc. Second Int. Workshop on Transforms and Filter Banks*, Brandenburg, Germany, March 1999, 51 pages
- It also shows how the general problem stated above can be solved conveniently.
- The formulas in the article are too complicated to go through in this course. A copy is available!
- In the sequel, we concentrate on defining the various types of two-channel filter banks and on giving some illustrative examples.

Qudrature Mirror Filter (QMF) Banks with Linear-Phase Subfilters

- For these filter banks,

$$G_1(z) = G_0(z) = \sum_{n=0}^{N_0} g_0[n] z^{-n}, \tag{23}$$

where N_0 is odd and $g_0[N_0 - n] = g_0[n]$ for $n = 0, 1, \cdots, (N_0-1)/2$.

- Hence, for the overall filter bank, there are only $(N_0+1)/2$ unknowns $g_0[n]$ for $n = 0, 1, \cdots, (N_0-1)/2$.
- In this case the overall transfer function $T(z)$ is given by

$$T(z) = [G_0(z)]^2 - [G_0(-z)]^2. \tag{24}$$

- The frequency response of the low-pass filter with the transfer function $G_0(z)$ is expressible as

$$G_0(e^{j\omega}) = e^{-j\omega N_0/2} \hat{G}_0(\omega), \tag{25a}$$

where

$$\hat{G}_0(\omega) = 2 \sum_{n=0}^{(N_0-1)/2} g_0[(N_0-1)/2 - n] \cos[(n+1/2)\omega]. \tag{25b}$$

- The overall frequency response can be written as

$$T(e^{j\omega}) = e^{-jN_0\omega} \hat{T}(\omega), \tag{26a}$$

where

$$\hat{T}(\omega) = [\hat{G}_0(\omega)]^2 + [\hat{G}_0(\omega + \pi)]^2. \tag{26b}$$

Optimization Problem

- For QMF banks, $\hat{T}(\omega)$ cannot be made equal to unity (PR solution) except for the trivial solution where $G_0(z) = (1+z^{-1})/2$ that does not provide good attenuation characteristics.
- The optimization problem can be stated as follows: Given an odd integer N_0 and $\rho > 0$ as well as δ_a, the maximum allowable reconstruction error, find the $(N_0+1)/2$ unknowns $g_0[n]$ of $G_0(z)$ to minimize

$$\varepsilon = \int_{\omega_s}^{\pi} [\hat{G}_0(\omega)]^2 \, d\omega \tag{27a}$$

subject to

$$\max_{\omega \in [0, \pi]} \left| [\hat{G}_0(\omega)]^2 + [\hat{G}_0(\omega + \pi)]^2 - 1 \right| \le \delta_a \tag{27b}$$

where $\hat{G}_0(\omega)$ is given by Equation (25b) and $\omega_s = (1+\rho)\pi/2$.

Comparisons

- For comparison purposes, we consider the designs of Johnston that is a real pioneer work of great value.
- Given ρ, α, and N_0, the quantity to be minimized in Johnston's technique is given by

$$E = E_1 + \alpha E_2, \tag{28a}$$

where

$$E_1 = \int_{\omega=0}^{\pi} \left([\hat{G}_0(\omega)]^2 + [\hat{G}_0(\omega + \pi)]^2 - 1 \right)^2 d\omega \tag{28b}$$

and

$$E_2 = \int_{\omega_s}^{\pi} [\hat{G}_0(\omega)]^2 \, d\omega \tag{28c}$$

with $\omega_s = (1+\rho)\pi/2$.

- Two designs, namely, $\rho = 0.172$, $\alpha = 2$, $N_0 = 31$; and $\rho = 0.172$, $\alpha = 5$, $N_0 = 63$, are compared with the proposed designs in Figure 6. The stopband edge is thus $\omega_s = 0.586\pi$.
- For the proposed designs, δ_a is selected to be equal to the maximum deviation of reconstruction error for Johnston's design. ($\delta_a = 3.23 \cdot 10^{-3}$ for the first design and $\delta_a = 7.03 \cdot 10^{-4}$ for the second design).
- As can be expected, the stop-band behaviors of the analysis filters in the proposed designs are significantly improved.
- Figures 7 and 8 give some more details for the proposed design with $N_0 = 63$.

Figure 6. Amplitude responses for the analysis filters in the proposed designs (solid line) and in Johnston's designs (dot-dashed line).

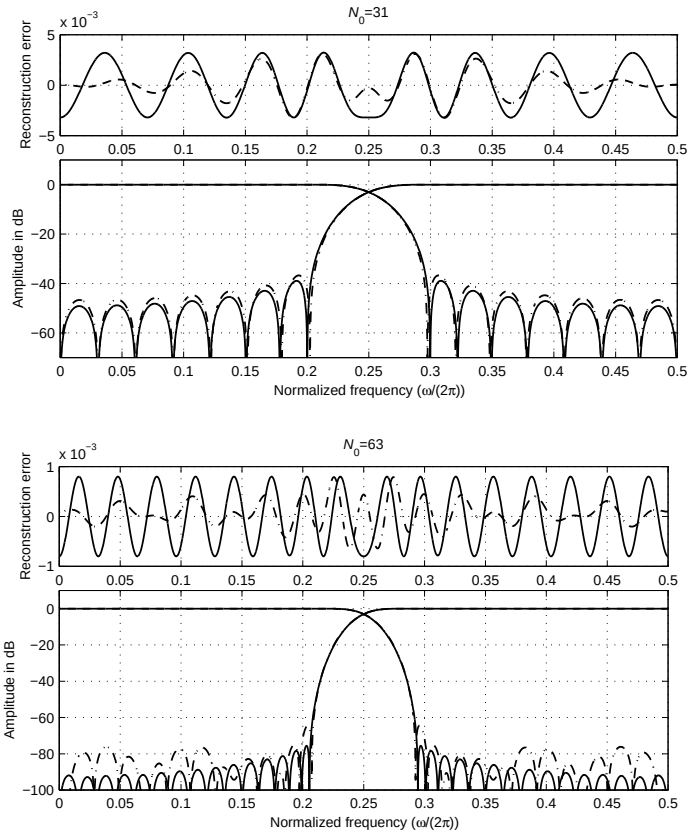

Figure 7. Amplitude responses for the analysis and synthesis filters for the proposed design with $N_0 = 63$.

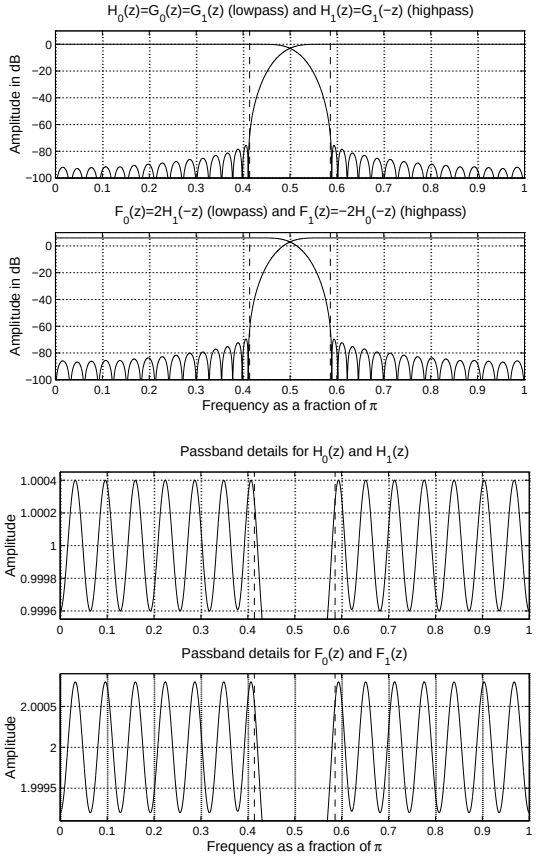

Figure 8. Impulse responses for the analysis and synthesis filters as well as the overall reconstruction error for the proposed design with $N_0 = 63$.

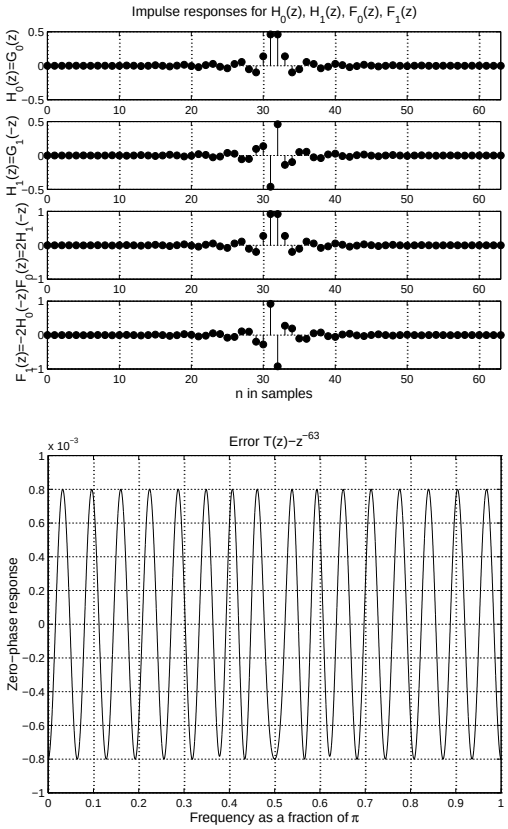

Low-Delay QMF Banks with Nonlinear-Phase Subfilters

- For these filter banks,

1. $G_1(z) = G_0(z) = \sum_{n=0}^{N_0} g_0[n] z^{-n}$, where N_0 is an odd integer.
2. $|G_0(e^{j\omega})|$ approximates zero on $[\omega_s, \pi]$, where $\omega_s = (1+\rho_s)\pi/2$ with $\rho_s > 0$, and unity on $[0, \omega_p]$, where $\omega_p = (1-\rho_p)\pi/2$ with $\rho_p > 0$.
3. $T(z) = [G_0(z)]^2 + [G_0(-z)]^2$ approximates the delay z^{-K} with K is being an odd integer satisfying $K < N_0$.

- The main purpose is to achieve a higher stopband attenuation for the same overall delay at the expense of increased filter orders.
- The impulse response of $G_0(z)$ cannot be symmetric so that all the impulse-response values $g_0[n]$ for $n = 0, 1, \cdots, N_0$ are unknowns.
- The second difference compared to the linear-phase case is that the overall distortion function is now given by

$$\left| T(e^{j\omega}) - e^{-jK\omega} \right| = \left| \left[G_0(e^{j\omega}) \right]^2 - \left[G_0(e^{j(\omega+\pi)}) \right]^2 - e^{-jK\omega} \right| . \quad (29)$$

- It is desired to make this function very small in the overall baseband $[0, \pi]$.
- The third difference, due to the nonlinear-phase characteristics, is that the performance of $G_0(z)$ in the passband must be controlled unlike for the linear-phase case.

Optimization Problem

- The optimization problem can be stated as follows: Given an odd order N_0, an odd integer $K < N_0$, ρ_s, ρ_p, δ_p, and δ_a, find the N_0+1 unknown impulse-response coefficients $g_0[n]$ of $G_0(z) = \sum_{n=0}^{N_0} g_0[n] z^{-n}$ to minimize

$$\varepsilon_0 = \int_{\omega_s}^{\pi} \left| G_0(e^{j\omega}) \right|^2 d\omega \quad (30a)$$

subject to

$$\max_{\omega \in [0,\pi]} \left| \left[G_0(e^{j\omega}) \right]^2 - \left[G_0(e^{j(\omega+\pi)}) \right]^2 - e^{-jK\omega} \right| \le \delta_a , \quad (30b)$$

$$\max_{\omega \in [0,\omega_p]} \left| \left| G_0(e^{j\omega}) \right| - 1 \right| \le \delta_p , \quad (30c)$$

and

$$\max_{\omega \in (\omega_p,\, \omega_s)} \left| G_0(e^{j\omega}) \right| - 1 \le \delta_p , \quad (30d)$$

where $\omega_p = (1-\rho_p)\pi/2$ and $\omega_s = (1+\rho_s)\pi/2$.

Example

- We consider the case where $\rho_s = \rho_p = 0.172$ ($\omega_s = 0.414\pi$ and $\omega_s = 0.586\pi$), $\delta_p = 0.01$, $\delta_a = 3.23\cdot 10^{-3}$, $N_0 = 63$, and $K = 31$.
- These are the same criteria as for the first linear-phase design of Figure 6 with the exception that now the sub-filter orders are increased from 31 to 63 while still achieving a delay of 31 samples.
- Figure 9 shows the amplitude responses for the analysis and the synthesis filters of the optimized design, whereas Figure 10 shows the corresponding impulse responses together with the reconstruction error.
- When comparing the analysis filters with those of the first filter bank of Figure 6, it is seen that the stopband attenuations are higher for the new design, as can be expected.
- It should be pointed out that in the passbands and in the transition bands the amplitude responses of the analysis filters stay well within the limit $1 \pm \delta_p$ with $\delta_p = 0.01$.

Figure 9. Amplitude responses for the analysis and synthesis filters for the proposed low-delay QMF bank with $N_0 = 63$ and $K = 31$.

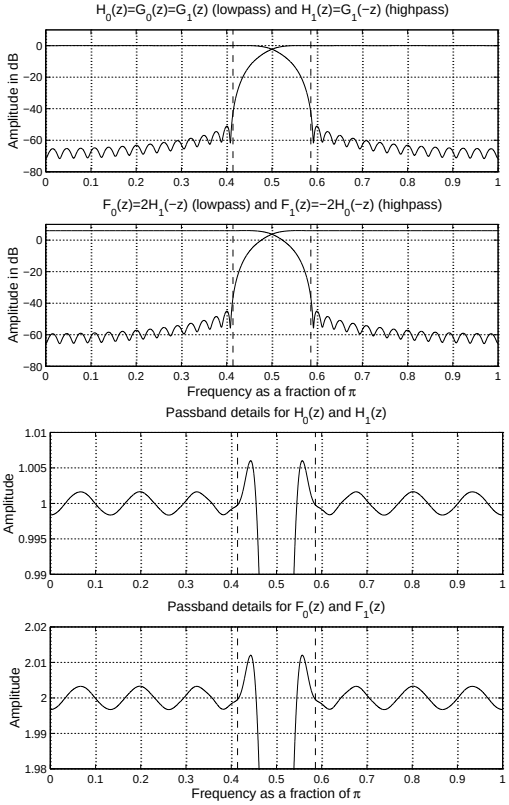

Figure 10. Impulse responses for the analysis and synthesis filters as well as the overall reconstruction error for the proposed low-delay QMF bank with $N_0 = 63$ and $K = 31$.

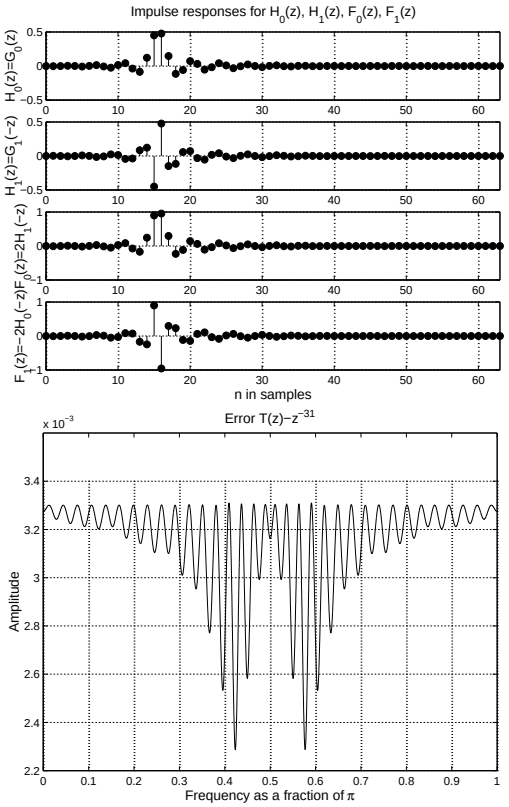

Orthogonal Filter Banks

- For these filter banks,

$$G_0(z) = \sum_{n=0}^{N_0} g_0[n] z^{-n}, \tag{31a}$$

where N_0 is an odd integer, and

$$G_1(z) = \sum_{n=0}^{N_1} g_1[n] z^{-n} = z^{-N_0} G_0\left(z^{-1}\right). \tag{31b}$$

In this case, the impulse-response coefficients of $G_1(z)$ are related to those of $G_0(z)$ via (see Figure 11)

$$g_1[n] = g_0[N_0 - n] \quad \text{for} \quad n = 0,1,\cdots,N_0. \tag{31c}$$

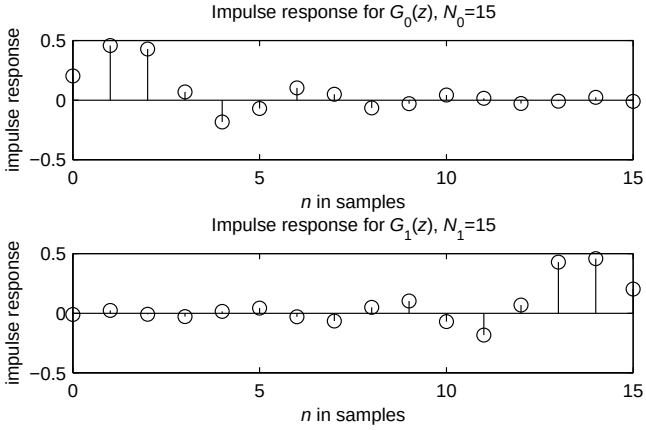

Figure 11. Relation between the impulse responses of $G_0(z)$ and $G_1(z)$.

- This makes the impulse responses of $G_0(z)$ and $G_1(z)$ time-reversed versions of each other and the filter orders N_0 and N_1 equal.
- It is well-known that filters having the time-reversed impulse responses also possess the same amplitude responses, that is, $|G_0(e^{j\omega})| = |G_1(e^{j\omega})|$.
- This fact also implies that the filter with transfer function $E(z) = G_0(z)G_1(z)$ is a linear-phase FIR filter of order $2N_0$ and having an impulse response of even symmetry.
- Furthermore, the frequency response of this filter is expressible as

$$E\left(e^{j\omega}\right) = e^{-jN_0\omega}\hat{E}(\omega), \tag{32a}$$

where

$$\hat{E}(\omega) = \left|G_0\left(e^{j\omega}\right)\right|^2 \equiv \left|G_1\left(e^{j\omega}\right)\right|^2. \tag{32b}$$

- This fact means that the zero-phase frequency response $\hat{E}(\omega)$ is non-negative.
- On the other hand, if $E(z)$ has a zero on the unit circle, then it is a double zero, making it separable into two filters having the same amplitude response and having the time-reversed impulse responses.
- Therefore, the following two conditions are required for $E(z)$ for being factorizable into $G_0(z)$ and $G_1(z)$ giving an orthogonal filter bank:

1. $E(z)$ is of the form $E(z) = \sum_{n=0}^{2N_0} e[n]z^{-n}$, where N_0 is odd, $e[N_0] = 1/2$, and $e[N_0 \pm 2r] = 0$ for $r = 1, 2, \cdots, (N_0-1)/2$, that is, $E(z)$ is a half-band filter of order $2N_0$.
2. The zero-phase frequency response of $E(z)$ is non-negative.

Mimax Design

- Based on the above facts, a two-channel orthogonal filter bank for the given odd order N_0 and for the stopband edge $\omega_s = (1+\rho)\pi/2$ with $\rho > 0$ can be accomplished as described in Part II of this course (Part II.F: Half-Band FIR Filters, Pages 234 –245).
- The main differences are the following:

1. Replace M by N_0.
2. Replace $T(z)$ by $G_0(z)$.
3. Replace $R(z)$ by $G_1(z)$.

- The amplitude responses of the resulting filters are orthogonal and exhibit an equiripple performance in both the stopband and passband.
- The basic factorization results in minimum-phase and maximum-phase transfer functions $G_0(z)$ and $G_1(z)$.
- By sharing the off-the-unit-circle zeros of $E(z)$ between $G_0(z)$ and $G_1(z)$ in a proper manner, mixed-phase filters can be generated with a rather linear-phase response in the passband.

Least-Squared Designs

- In this case optimization is required and the problem can be stated as follows: Given an odd order N_0 and $\rho > 0$, find the impulse-response coefficients of $G_0(z) = \sum_{n=0}^{N_0} g_0[n]z^{-n}$ to minimize

$$\varepsilon_0 = \int_{\omega_s}^{\pi} \left|G_0\left(e^{j\omega}\right)\right|^2 d\omega, \tag{33a}$$

where

$$\omega_s = (1+\rho)/2 \tag{33b}$$

subject to the condition that the product of the transfer functions $G_0(z) = \sum_{n=0}^{N_0} g_0[n]z^{-n}$ and $G_1(z) = \sum_{n=0}^{N_0} g_0[N_0 - n]z^{-n}$ is a linear-phase half-band filter of order $2N_0$.

Examples

- $\rho = 0.172$ is used for determining the edges of the filters in the two-channel filter bank under the consideration.
- The stopband edge of $G_0(z)$ is thus located at $\omega_s = (1+\rho)\pi/2 = 0.586\pi$.
- As examples, Figure 12 compares the minimax and the least-squared designs in the $N_0 = 31$ and $N_0 = 63$ cases, respectively.
- As can be expected, the attenuations provided by the least-squared filters are lower near the stopband edges, but become higher for frequencies further away from the edge frequencies.
- Figures 13 and 14 show more details in the $N_0 = 63$ case.
- Notice the extremely small passband ripples in the passband regions with passband edges being located at $\omega = (1 - \rho)\pi/2 = 0.414\pi$ and $\omega = (1 + \rho)\pi/2 = 0.586\pi$.

Figure 12. Amplitude responses for the analysis filters designed in the least mean-square sense (solid line) and in the minimax sense (dot-dashed line).

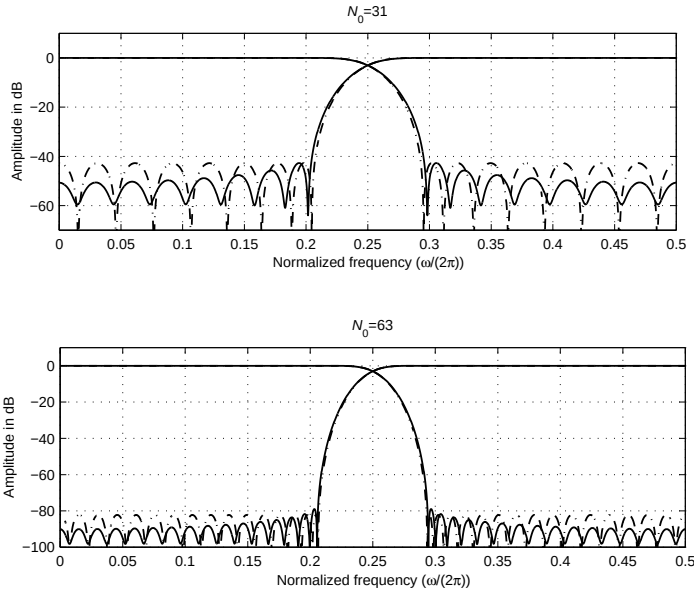

Figure 13. Amplitude responses for the analysis and synthesis filters for the example PR orthogonal filter banks with $N_0 = 63$. The solid and dashes lines are for the least-squared and minimax designs, respectively.

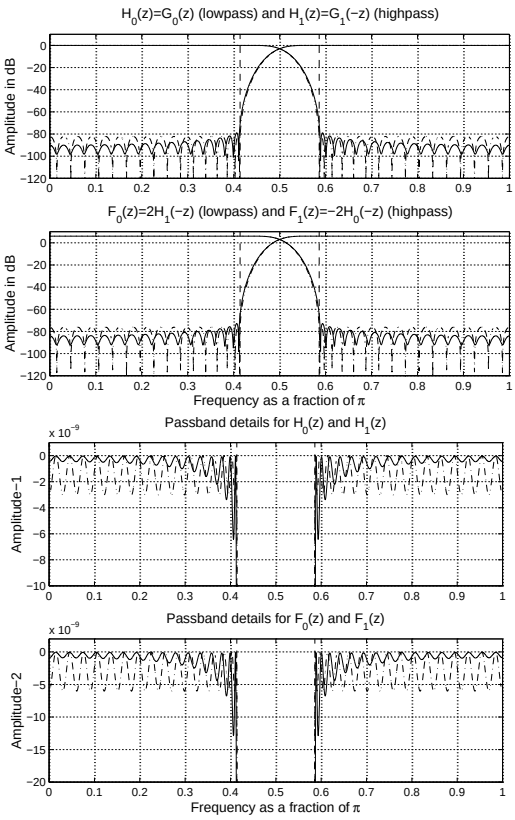

Figure 14. Impulse responses for the analysis and synthesis filters. The first and second figures are for the least-squared and minimax designs, respectively.

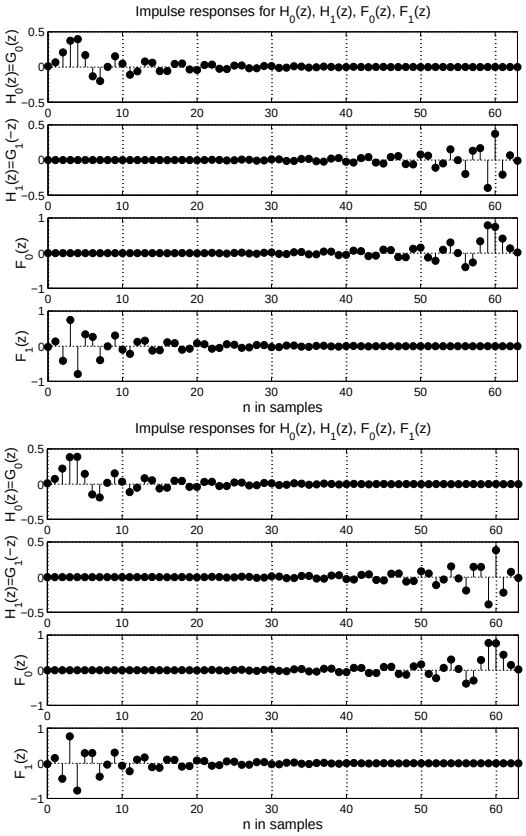

PR Biorthogonal Filter Banks with Linear-Phase Subfilters

- For these filter banks, $G_0(z) = \sum_{n=0}^{N_0} g_0[n] z^{-n}$ and $G_1(z) = \sum_{n=0}^{N_1} g_1[n] z^{-n}$ satisfy the following conditions:

1. The impulse responses of $G_0(z)$ and $G_1(z)$ possess an even symmetry, that is, $g_0[N_0 - n] = g_0[n]$ for $n = 0, 1, \cdots, N_0$ and $g_1[N_1 - n] = g_1[n]$ for $n = 0, 1, \cdots, N_1$.
2. The sum of the filter orders N_0 and N_1 is two times an odd integer, that is, $N_0 + N_1 = 2K$ with K being an odd integer.
3. $E(z) = G_0(z)G_1(z)$ is a half-band FIR filter of order $N_0 + N_1$.

- There exist only the following two cases to meet these conditions:
  - *Type A:* N_0 and N_1 are odd integers and their sum is two times an odd integer K.
  - *Type B:* N_0 and N_1 are even integers and their sum is two times an odd integer K.
- In both cases, the overall filter bank delay is an odd integer given by $K = (N_0 + N_1)/2$.

- For both Type A and B, the frequency responses of $G_k(z)$ for $k = 0, 1$ are expressible as

$$G_k\left(e^{j\omega}\right) = e^{-j\omega N_k/2} \hat{G}_k(\omega) \tag{34a}$$

where

$$\hat{G}_k(\omega) = \begin{cases} 2 \sum_{n=0}^{(N_k-1)/2} g_k[(N_k-1)/2 - n][\cos[(n+1/2)\omega]] \\ \qquad \text{for Type A} \\ g_k[N_k/2] + 2 \sum_{n=1}^{N_k/2} g_k[N_k/2 - n][\cos[n\omega]] \\ \qquad \text{for Type B.} \end{cases} \tag{34b}$$

- The optimization of PR biorthogonal banks is very complicated due to the fact that $G_0(z)$ and $G_1(z)$ are different transfer functions.
- They are only connected together through the fact that $G_0(z)G_1(z)$ should be a linear-phase half-band filter.

Optimization Problem:

For both Types A and B, we state the problem in the following form: Given the filter type, N_0, N_1, $\rho_p^{(k)}$ and $\rho_s^{(k)}$ for $k = 0$, 1, and δ_p, find the adjustable coefficients of $G_0(z)$ and $G_1(z)$, to minimize

$$\varepsilon = \max(\varepsilon_0, \varepsilon_1), \tag{35a}$$

where

$$\varepsilon_k = \int_{\omega_s^{(k)}}^{\pi} \left[\hat{G}_k(\omega)\right]^2 d\omega \quad \text{for} \quad k = 0,1, \tag{35b}$$

subject to

$$\max_{\omega \in [0,\pi]} \left| \hat{G}_0(\omega)\hat{G}_1(\omega) + \hat{G}_0(\pi - \omega)\hat{G}_1(\pi - \omega) - 1 \right| = 0, \tag{35c}$$

$$\max_{\omega \in [0, \omega_p^{(k)}]} \left| \hat{G}_k(\omega) - 1 \right| \le \delta_p \quad \text{for} \quad k = 0,1, \tag{35d}$$

$$\max_{\omega \in (\omega_p^{(k)}, \omega_s^{(k)})} \hat{G}_k(\omega) - 1 \le \delta_p \quad \text{for} \quad k = 0,1. \tag{35e}$$

- Here, $\omega_s^{(k)} = (1 + \rho_s^{(k)})\pi/2$ and $\omega_p^{(k)} = (1 - \rho_p^{(k)})\pi/2$ for $k =$ 0,1 and $\hat{G}_0(\omega)\hat{G}_1(\omega) + \hat{G}_0(\pi - \omega)\hat{G}_1(\pi - \omega)$ the zero-phase frequency response for the overall system of Figure 1.
- For the PR case, this should be identical equal to unity in the overall frequency band.

Example

- This example emphasizes the importance of the optimization problem formulation in order to achieve PR linear-phase biorthogonal banks with good selectivity properties.
- As examples we consider the design of filters in the $N_0 = N_1 = 31$ case and in the $N_0 = N_1 = 63$ case for $\rho_p^{(k)} = \rho_s^{(k)} = 0.172$ for $k = 0,1$.
- The resulting passband and stopband edges for both $G_0(z)$ and $G_1(z)$ are thus located at $\omega_p = 0.414\pi$ and $\omega_s = 0.586\pi$, respectively.
- In both cases, two problem formulations have been used.
- In the first formulation, the error function under consideration is given (Vaidyanathan and Nguen) by

$$\begin{aligned} E = & \int_{\omega=\omega_s^{(0)}}^{\pi} \left[\hat{G}_0(\omega)\right]^2 d\omega + \int_{\omega=\omega_s^{(1)}}^{\pi} \left[\hat{G}_1(\omega)\right]^2 d\omega \\ & + \int_{\omega=0}^{\omega_p^{(0)}} \left[\hat{G}_0(\omega) - 1\right]^2 d\omega + \int_{\omega=0}^{\omega_p^{(1)}} \left[\hat{G}_1(\omega) - 1\right]^2 d\omega. \end{aligned} \tag{36}$$

- For the second formulation, the proposed formulation is used with $\delta_p = 0.17$ (a 3-dB peak-to-peak passband ripple).
- Figure 15 shows that the second problem formulation results in analysis filters having significantly higher stopband attenuations.

- Figures 16 and 17 show more details for the proposed design with $N_0 = N_1 = 63$. For this design there is a too large over-shoot in the transition band.
- This is because the transition band behavior was not under consideration when optimizing the filter bank.
- The overall reconstruction error is extremely small (zero in theory) and is not shown in the figures.

Figure 15. Amplitude responses for the analysis filters designed using the proposed technique (solid line) and the the technique of Vaidyanathan and Nguen(dot-dashed line).

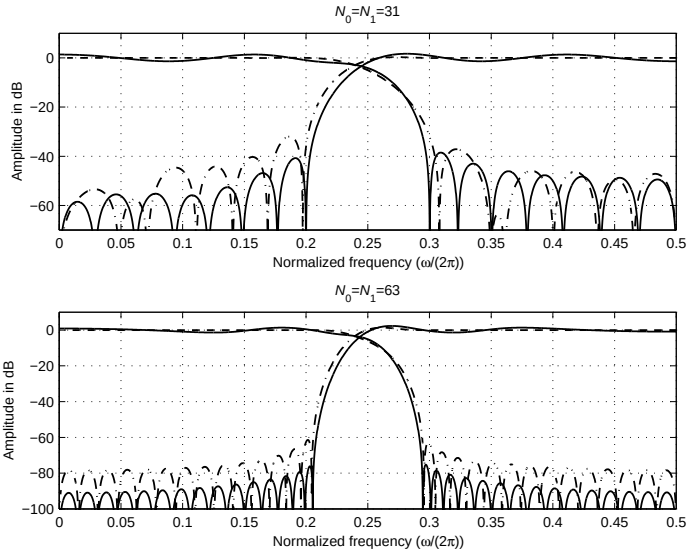

Figure 16. Amplitude responses for the analysis and synthesis filters for the example biorthogonal PR filter bank with $N_0 = N_1 = 63$.

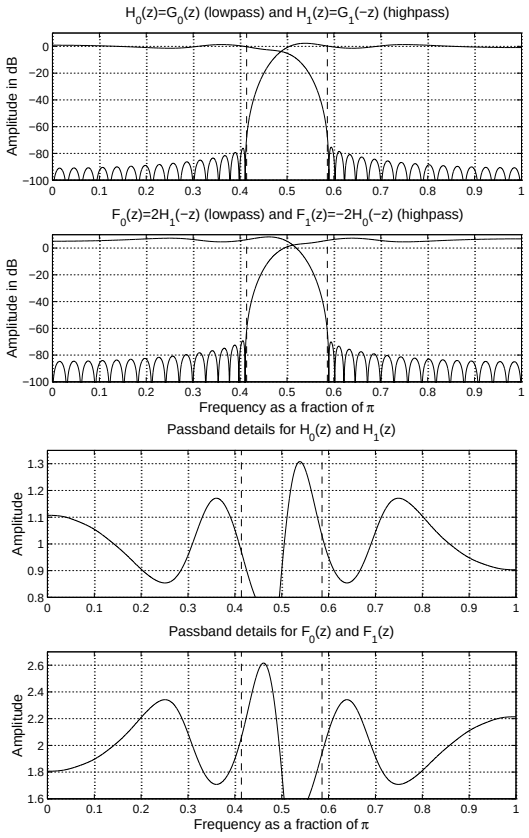

Figure 17. Impulse responses for the analysis and synthesis filters.

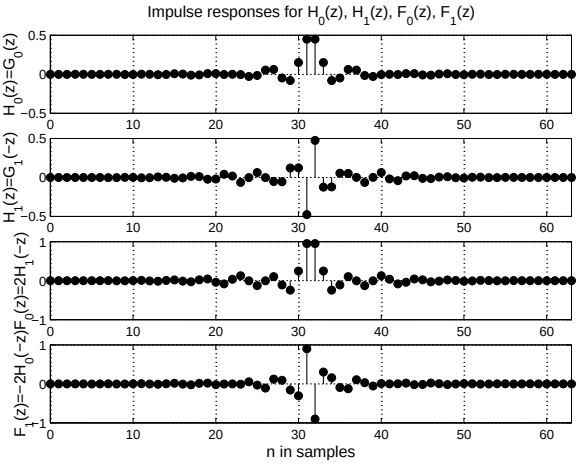

Problem of selecting the orders of $G_0(z)$ and $G_1(z)$

- As mentioned above, the overall delay K is related to the subfilter orders N_0 and N_1 by $K = (N_0 + N_1)/2$.
- The same delay is obtained by different selections of N_0 and N_1 and it is desired to find the selection minimizing the maximum of the stopband energies of the two subfilters.
- As an example, we consider the case where $K = 31$ and $\rho_p^{(k)} = \rho_s^{(k)} = 0.172$ for $k = 0, 1$.
- The resulting passband and stopband edges for both $G_0(z)$ and $G_1(z)$ are thus $\omega_p = 0.414\pi$ and $\omega_s = 0.586\pi$.
- For $K = 31$, the desired delay is obtained by selecting N_0 and N_1 as $N_0 = 31 - l$ and $N_1 = 31 + l$ for $l = 0, 1, \cdots, 30$.
- Three groups of filters have been optimized to minimize the maximum of the stopband energies of $G_0(z)$ and $G_1(z)$.
- For these groups, the passband ripples are 0.01, 0.05, and 0.1, respectively.
- For each group, N_0 varies from 17 to 31 and $N_1 = 62 - N_0$.
- Some of the properties of the optimized filter banks are summarized in Figure 18.
- The upper part shows for the three different values of the passband ripple the maximum of the stopband energies of $G_0(z)$ and $G_1(z)$.
- The lower part, in turn, shows the attenuations of both $G_0(z)$ and $G_1(z)$ at the frequency point where the first stopband maximum occurs.

Figure 18. Dependences of the stopband behaviors of $G_0(z)$ and $G_1(z)$ on N_0 and the passband ripple δ_p [δ_p = 0.1(x), 0.05(o), 0.01(*)] for PR biorthogonal filter banks with $K = (N_0 + N_1)/2 = 31$.

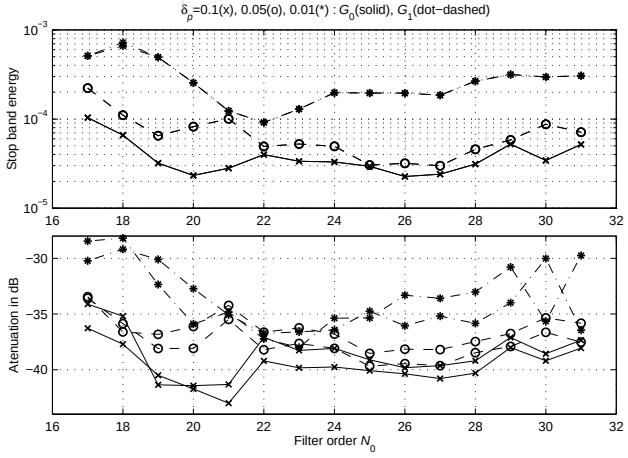

- Note that the attenuation of $G_0(z)$ and $G_1(z)$ are different.
- Therefore, there are two curves, the first one corresponding to $G_0(z)$ and the second one to $G_1(z)$.
- There is an error on the top of the figure: delete 'G_0 (solid), G_0 (solid)'.

- Two interesting observations can be made.
- First, the stopband behaviors of the two subfilters depends strongly on the given passband ripple.
- If the allowed ripple is higher, filters with improved stopband performances are achieved.
- Second, it is not straightforward to find the value of N_0 that gives the best stopband performances for the two subfilters.
- Furthermore, the best value of N_0 depends on the given allowable passband ripple.
- For $\delta_p = 0.1$, $\delta_p = 0.05$, and $\delta_p = 0.01$, the best results are achieved by $N_0 = 20$ and $N_1 = 42$; $N_0 = 27$ and $N_1 = 35$; and $N_0 = 22$ and $N_1 = 40$, respectively.
- Therefore, the filter orders to give the desired overall delay with the minimized stopband energy can be found only by going through all possible order combinations.

Low-Delay PR Biorthogonal Filter Banks with Nonlinear-Phase Subfilters

- For these filter banks, $G_0(z) = \sum_{n=0}^{N_0} g_0[n] z^{-n}$ and $G_1(z) = \sum_{n=0}^{N_1} g_1[n] z^{-n}$ satisfy the following conditions:

1. The impulse responses of $G_0(z)$ and $G_1(z)$ are not symmetric.
2. The impulse response of $E(z) = G_0(z)G_1(z) = \sum_{n=0}^{N_0+N_1} e[n] z^{-n}$ satisfies

$$e[n] = \begin{cases} 1/2 & \text{for } n = K \\ 0 & \text{for } n \text{ is odd and } n \neq K, \end{cases} \tag{37}$$

where K is an odd integer with $K < (N_0 + N_1)/2$.

- An example for an impulse response of $E(z)$ is shown in Figure 4(b) of Page 23.
- The second condition implies that the overall transfer function between the output and input is $T(z) = z^{-K}$ with K less than $(N_0 + N_1)/2$ and the sum of the orders must be two times an odd integer L.
- Since the overall system delay is less than half the sum of the filter orders, the impulse responses of $G_0(z)$ and $G_1(z)$ cannot possess an even symmetry.
- The high number of unknowns (altogether N_0+N_1+2) and the PR condition with the delay less than half the sum of the filter orders makes the synthesis of the overall system very nonlinear and complicated.

Optimization Problem:

Given N_0, N_1, $\rho_p^{(k)}$ and $\rho_s^{(k)}$ for $k = 0$, 1, and δ_p as well as K, find the adjustable coefficients of $G_0(z)$ and $G_1(z)$ to minimize

$$\varepsilon = \max(\varepsilon_0, \varepsilon_1), \tag{38a}$$

where

$$\varepsilon_k = \int_{\omega_s^{(k)}}^{\pi} \left| G_k\left(e^{j\omega}\right) \right|^2 d\omega \quad \text{for} \quad k = 0,1, \tag{38b}$$

subject to

$$\max_{\omega \in [0,\pi]} \left| T\left(e^{j\omega}\right) - e^{-jK\omega} \right| = 0, \tag{38c}$$

$$\max_{\omega \in \left[0, \omega_p^{(k)}\right]} \left| \left| G_k\left(e^{j\omega}\right) \right| - 1 \right| \le \delta_p \quad \text{for} \quad k = 0, 1, \tag{38d}$$

and

$$\max_{\omega \in \left(\omega_p^{(k)}, \omega_s^{(k)}\right)} \left| G_k\left(e^{j\omega}\right) \right| - 1 \le \delta_p \quad \text{for} \quad k = 0,1. \tag{38e}$$

Here, $\omega_s^{(k)} = (1+\rho_s^{(k)})\pi/2$ and $\omega_p^{(k)} = (1-\rho_p^{(k)})\pi/2$ for $k = 0,1$ and $T\left(e^{j\omega}\right) = G_0\left(e^{j\omega}\right)G_1\left(e^{j\omega}\right) - G_0\left(e^{j(\omega+\pi)}\right)G_1\left(e^{j(\omega+\pi)}\right)$ is the frequency response for the overall system of Figure 1. In the PR case it should be equal to $e^{-jK\omega}$ in the overall frequency range.

Examples

- It is desired to design low-delay PR biorthogonal filter banks for K = 31, δ_p = 0.01, and $\rho_p^{(k)} = \rho_s^{(k)} = 0.172$ for $k = 0,1$.
- The passband and stopband edges for both $G_0(z)$ and $G_1(z)$ are thus located at $\omega_p = 0.414\pi$ and $\omega_s = 0.586\pi$.
- Figure 19 compares the optimized low-delay PR filter banks with the biorthogonal filter bank with linear phase subfilters of orders $N_1 = N_0 = 31$ in the $N_1 = N_0 = 33$, $N_1 = N_0 = 45$, and $N_1 = N_0 = 63$ cases.
- As can be expected, the stopband attenuations of the analysis filters in the low-delay filter banks increase when the filter orders are increased.
- Figures 20 and 21 show more details for the proposed design with $N_0 = N_1 = 45$.

Figure 19. Comparisons between low-delay biorthogonal filters banks (solid lines) in the K=31 case with the linear-phase biorthogonal case (dot-dashed lines).

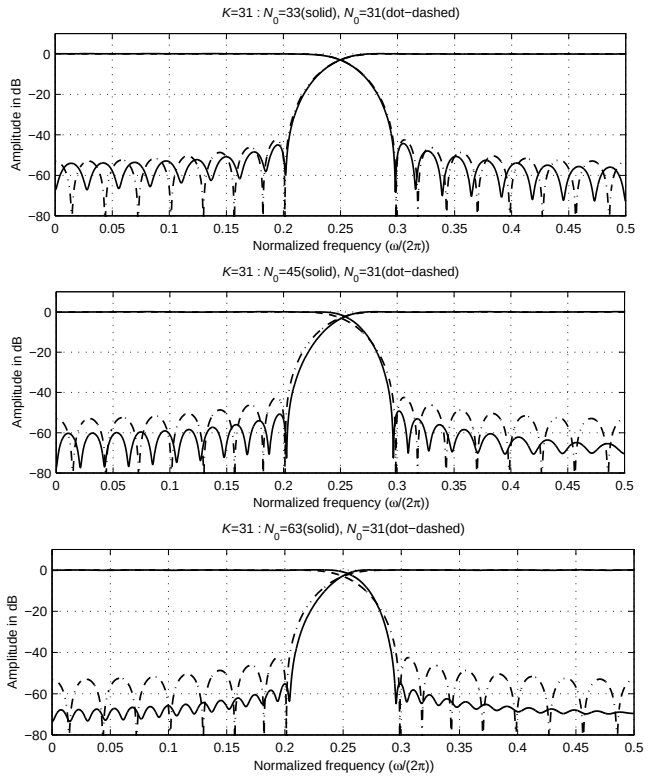

Figure 20. Amplitude responses for the analysis and synthesis filters for the example low-delay biorthogonal PR filter bank with $N_0 = N_1 = 45$.

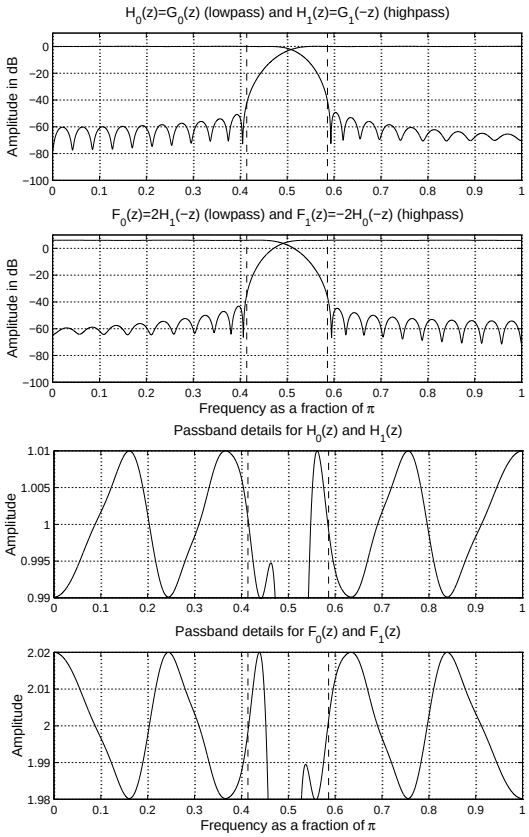

Figure 21. Impulse responses for the analysis and synthesis filters.

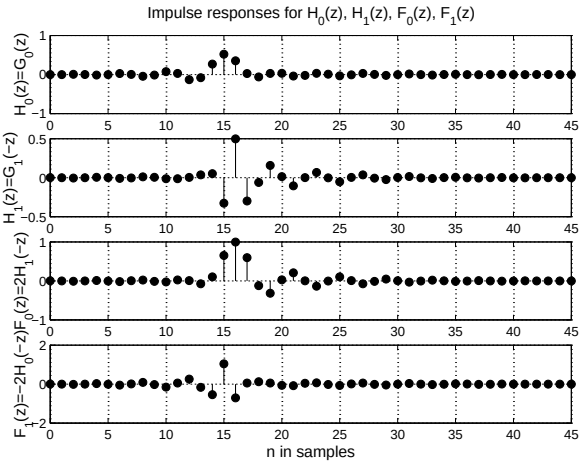

NPR Biorthogonal Filter Banks with Linear-Phase Subfilters

- For these filter banks, $G_0(z) = \sum_{n=0}^{N_0} g_0[n] z^{-n}$ and $G_1(z) = \sum_{n=0}^{N_1} g_1[n] z^{-n}$ satisfy the following conditions:

1. The impulse responses of $G_0(z)$ and $G_1(z)$ possess an even symmetry, that is, $g_0[N_0 - n] = g_0[n]$ for $n = 0, 1, \cdots, N_0$ and $g_1[N_1 - n] = g_1[n]$ for $n = 0, 1, \cdots, N_1$.
2. The sum of the filter orders N_0 and N_1 is two times an odd integer, that is, $N_0 + N_1 = 2K$ with K being an odd integer.
3. $E(z) = G_0(z)G_1(z) = \sum_{n=0}^{N_0+N_1} e[n] z^{-n}$ is nearly a half-band FIR filter of order $N_0 + N_1$, that is, its impulse-response coefficients satisfy

$$e[n] \approx \begin{cases} 1/2 & \text{for } n = K \\ 0 & \text{for } n \text{ is odd and } n \neq K, \end{cases} \tag{39}$$

where $K = (N_0 + N_1)/2$.

- The main difference compared to the corresponding PR case considered earlier is that now the overall transfer function $T(z)$ approximates the delay term z^{-K} and there is some amplitude distortion.
- The optimization problem is also the same except that the condition of Eq. (35c) is replaced by

$$\max_{\omega \in [0,\pi]} \left| \hat{G}_0(\omega)\hat{G}_1(\omega) + \hat{G}_0(\pi - \omega)\hat{G}_1(\pi - \omega) - 1 \right| \leq \delta_a, \tag{40}$$

where δ_a is the allowable amplitude distortion.

Examples

- Several NPR biorthogonal two-channel filter banks with linear-phase subfilters of orders $N_1 = N_0 = 31$ have been optimized for $\rho_p^{(k)} = \rho_s^{(k)} = 0.172$ for $k = 0, 1$.
- The passband and stopband edges for both $G_0(z)$ and $G_1(z)$ are thus located at $\omega_p = 0.414\pi$ and $\omega_s = 0.586\pi$.
- These filters have been optimized for various values of the reconstruction error δ_a and for three values of the passband ripple, namely, $\delta_p = 0.1$, $\delta_p = 0.01$, and $\delta_p = 0.001$.
- Figure 22 shows the amplitude responses of the analysis filters in the $\delta_p = 0.1$ case for $\delta_a = 0.00001$ and $\delta_a = 0.001$. Also, the overall amplitude distortions are shown in the figure.
- Figures 23 and 24 show more details in the $\delta_a = 0.001$ case.
- Figure 25 illustrates the dependence of the stopband behaviors of $G_0(z)$ and $G_1(z)$ on the reconstruction error and the passband ripple.
- It is interesting to observe that the stopband behaviors of the two subfilters become almost the same for the reconstruction errors smaller than 10^{-5}.
- On the other hand, when the passband ripple is increased, the stopband attenuations increase significantly.
- It is also interesting to observe that for large allowable reconstruction errors, the filter attenuations increase and the dependence on the passband ripple decreases.

Figure 22. Biorthogonal NPR linear-phase filter banks with small reconstruction error for $N_1 = N_0 = 31$ and $\delta_p = 0.1$. The solid and dot-dashed lines give the amplitude responses of analysis filters and the reconstruction errors for $\delta_a = 0.001$ and $\delta_a = 0.00001$, respectively.

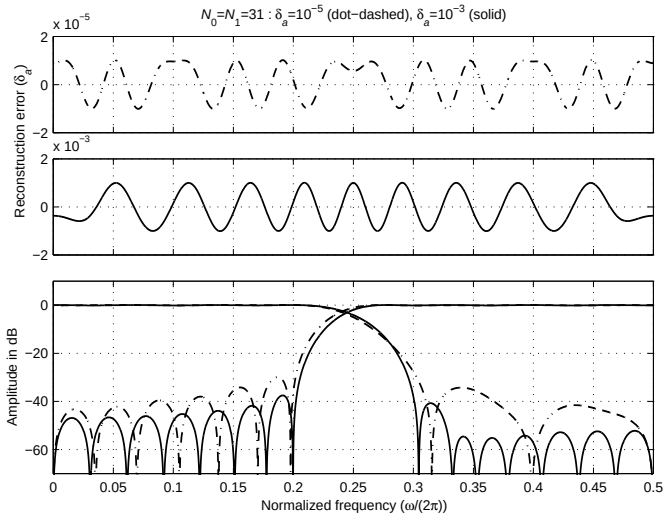

Figure 23. Amplitude responses for the analysis and synthesis filters for the example NPR biorthogonal filter bank with linear-phase subfilters.

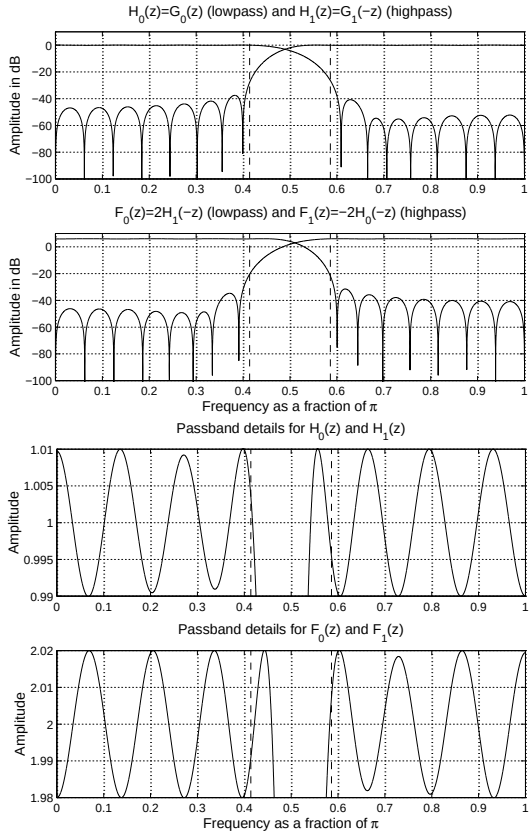

Figure 24. Impulse responses for the analysis and synthesis filters as well as the overall reconstruction error for the example NPR biorthogonal filter bank .

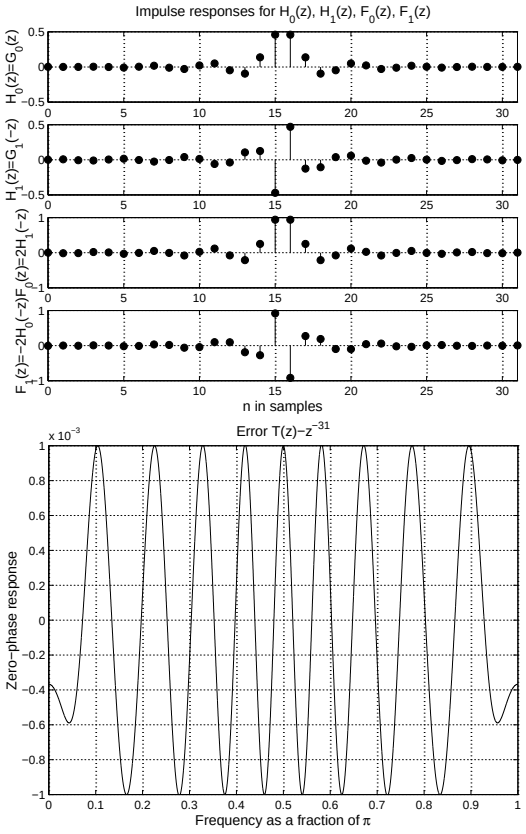

Figure 25. Dependences of the stopband behaviors of $G_0(z)$ and $G_1(z)$ on the reconstruction error δ_a and the passband ripple δ_p [δ_p = 0.1(x), 0.01(o), 0.001(*)] for NPR linear-phase biorthogonal filter banks with $N_0 = N_1 = 31$.

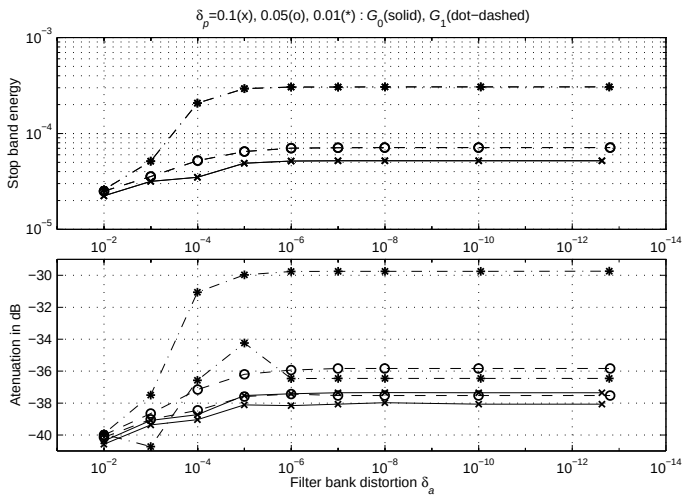

- The upper part shows in each case the maximum of the stopband energies of $G_0(z)$ and $G_1(z)$.
- The lower part, in turn, shows the attenuations of both $G_0(z)$ and $G_1(z)$ at the frequency point where the first stopband maximum occurs.
- Since these attenuation values are different for $G_0(z)$ and $G_1(z)$, two curves are given in each case.
- Notice the same error as in Figure 18.

Low-Delay NPR Biorthogonal Filter Banks with Nonlinear-Phase Subfilters

- For these filter banks, $G_0(z) = \sum_{n=0}^{N_0} g_0[n] z^{-n}$ and $G_1(z) = \sum_{n=0}^{N_1} g_1[n] z^{-n}$ satisfy the following conditions:

1. The impulse responses of $G_0(z)$ and $G_1(z)$ are not symmetric.
2. The sum of the filter orders N_0 and N_1 is two times an odd integer.
3. The impulse response of $E(z) = G_0(z)G_1(z) = \sum_{n=0}^{N_0+N_1} e[n] z^{-n}$ satisfies

$$e[n] \approx \begin{cases} 1/2 & \text{for } n = K \\ 0 & \text{for } n \text{ is odd and } n \neq K, \end{cases} \tag{41}$$

where $K < (N_0 + N_1)/2$.

- The difference compared to the corresponding low-delay PR case is again that now $T(z)$ approximates the delay term z^{-K} and there is some amplitude and phase distortion.
- The optimization problem is also the same except that the condition of Eq. (38c) is replaced by

$$\max_{\omega \in [0,\pi]} \left| G_0\left(e^{j\omega}\right) G_1\left(e^{j\omega}\right) - G_0\left(e^{j(\omega+\pi)}\right) G_1\left(e^{j(\omega+\pi)}\right) - e^{-jK\omega} \right| \leq \delta_a, \tag{42}$$

where δ_a is the allowable distortion.

Example

- Several NPR low-delay biorthogonal two-channel filter banks with nonlinear-phase subfilters of orders $N_1 = N_0 = 31$ have been designed for $K = 31$ and for various reconstruction errors.
- Like in earlier examples, the passband and stopband edges for both $G_0(z)$ and $G_1(z)$ are again located at $\omega_p = 0.414\pi$ and $\omega_s = 0.586\pi$, respectively.
- Since $N_1 = N_0 = K = 31$, the resulting filter banks are automatically NPR orthogonal banks provided that the allowable passband ripple in the optimization is large enough.
- Figure 26 shows the amplitude responses of the analysis filters in the $\delta_p = 0.1$ case for $\delta_a = 0.00001$ and $\delta_a = 0.001$. Also, the overall amplitude distortions are shown in the figure.
- Figure 27 illustrates the dependence of the stopband behaviors of $G_0(z)$ and $G_1(z)$ on the reconstruction error.
- It is interesting to notice that the filter attenuations are almost the same for the reconstruction errors smaller than 10^{-5}.
- Only for large reconstruction errors, a higher attenuation is achieved.
- The passband ripple depends directly on other filter bank properties.

Figure 27. Orthogonal NPR filter banks with small reconstruction error for $N_1 = N_0 = K=31$ and $\delta_p = 0.1$. The solid and dot-dashed lines give the amplitude responses of analysis filters and the reconstruction errors for $\delta_a = 0.001$ and $\delta_a = 0.00001$, respectively.

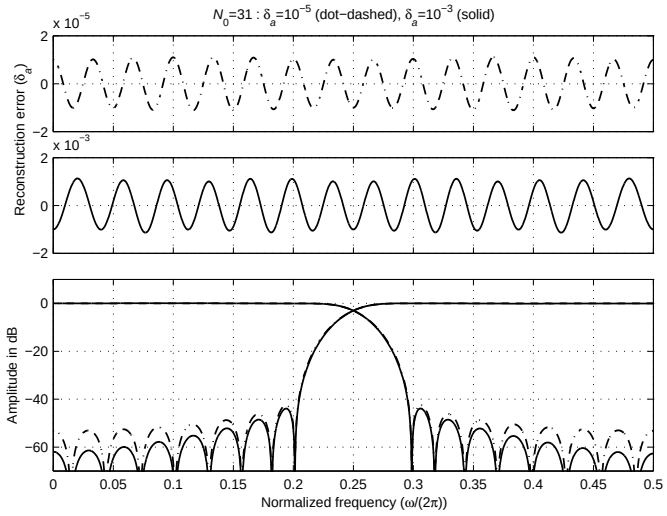

Figure 27. Dependences of the stopband behaviors of $G_0(z)$ and $G_1(z)$ on the reconstruction error δ_a for NPR orthogonal filter banks with $N_0 = N_1 = 31$.

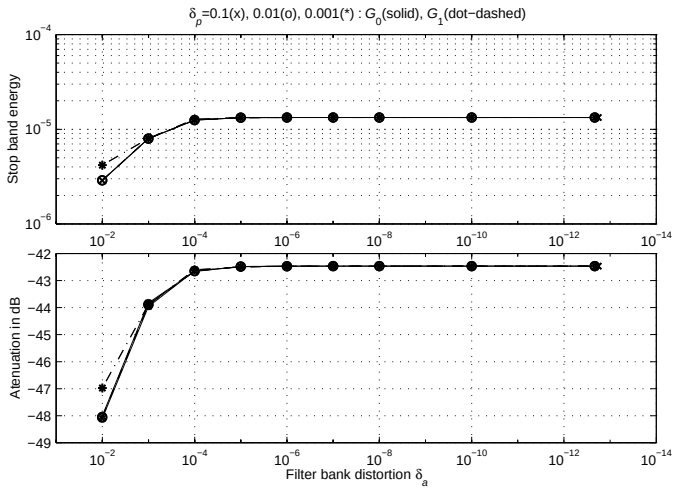

- The upper part shows in each case the maximum of the stopband energies of $G_0(z)$ and $G_1(z)$.
- The lower part, in turn, shows the attenuations of both $G_0(z)$ and $G_1(z)$ at the frequency point where the first stopband maximum occurs. In this case the attenuation are the same for both $G_0(z)$ and $G_1(z)$.
- Notice the same error as in Figures 18 and 25.

Another example

- Several NPR low-delay biorthogonal two-channel filter banks with nonlinear-phase subfilters have been designed for the overall delay $K = 31$ and for various reconstruction errors and passband ripples.
- The passband and stopband edges for $G_0(z)$ and $G_1(z)$ are the same as in earlier examples.
- Two different subfilter orders are considered, namely, $N_0 = N_1 = 33$ and $N_0 = N_1 = 63$.
- Figure 28 shows in these two cases amplitude characteristics of the analysis filters and the reconstruction errors for $\delta_p = 0.01$ and $\delta_a = 10^{-5}$.
- Figures 29 and 30 illustrate the dependence of the stopband behaviors of $G_0(z)$ and $G_1(z)$ on the reconstruction error and the passband ripple for $N_1 = N_0 = 33$ and $N_1 = N_0 = 63$, respectively.

Figure 28. Low-delay filter banks for $K = 31$, $\delta_p = 0.01$, and $\delta_a = 10^{-5}$. The solid and dot-dashed lines give the amplitude responses of analysis filters and the reconstruction errors for $N_1 = N_0 = 63$ and $N_1 = N_0 = 31$, respectively.

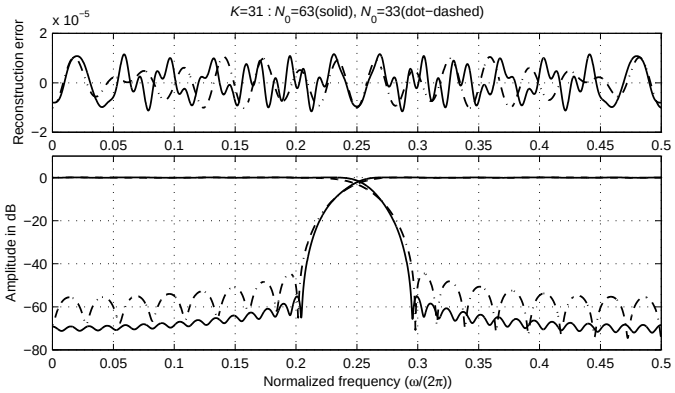

Figure 29. Dependences of the stopband behaviors of $G_0(z)$ and $G_1(z)$ on the reconstruction error δ_a and the passband ripple δ_p [$\delta_p = 0.1$(x), 0.01(o), 0.001(∗)] for NPR nonlinear-phase biorthogonal filter banks with $N_0 = N_1 = 33$ for $K = 31$.

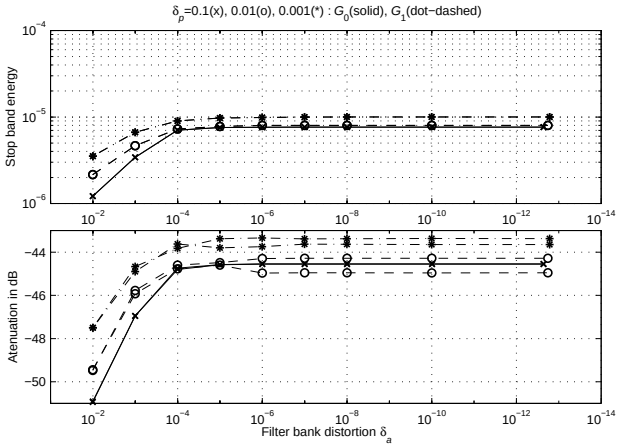

- The upper part shows in each case the maximum of the stopband energies of $G_0(z)$ and $G_1(z)$.
- The lower part, in turn, shows the attenuations of both $G_0(z)$ and $G_1(z)$ at the frequency point where the first stopband maximum occurs.
- Since these attenuation values are different for $G_0(z)$ and $G_1(z)$, two curves are given in each case. Notice the same error as in Figures 18, 25, and 27.

Figure 30. Dependences of the stopband behaviors of $G_0(z)$ and $G_1(z)$ on the reconstruction error δ_a and the passband ripple δ_p [$\delta_p = 0.1$(x), 0.01(o), 0.001(∗)] for NPR nonlinear-phase biorthogonal filter banks with $N_0 = N_1 = 63$ for $K = 31$.

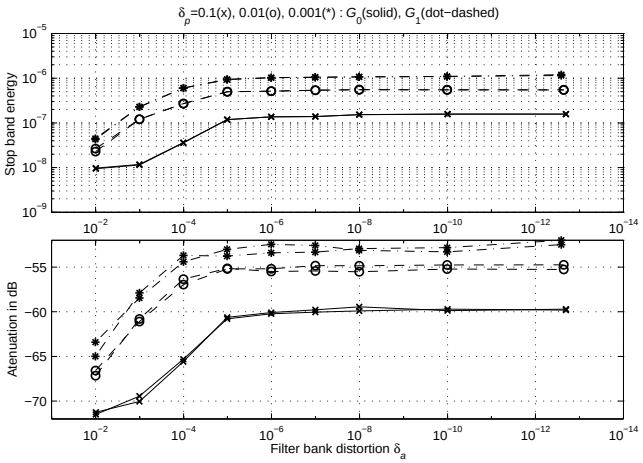

- The comments given after Figure 29 are also valid after Page 30.

Comments

- The practical implementation issues have been totally omitted in this pile of lecture notes.
- They will be added in the next version.
- If there is a need to know about alternative implementation form, please contact the lecturer.
- He has also plenty of FORTRAN and MATLAB files.
- The reason for such a long pile of lecture notes on two-channel FIR filter banks is due to the fact that Robert Bregović and the lecturer have written the tutorial article mentioned on Page 7.
- Many thanks to Robert in helping in prepapring Part V.A.

Part V.B: Two-Channel IIR Filter Banks

- This part shows how to generate two-channel IIR filter banks using half-band IIR filters.
- These filters were considered earlier in details in Part II, namely, Part II.G: Half-Band IIR Filters (Pages 246-266 in Part II).
- There are also other types of two-channel IIR filter banks.
- If there is some interest, please contact the lecturer. He is able to give some extra material.
- It should be pointed out that there is one project going on at the Signal Processing Laboratory regarding these filter banks. The results will appear in the next version of this pile of lecture notes.
- We concentrate on the following two topics:

I. Two-Channel IIR Filter Banks with Phase Distortion. These banks are generated directly by using half-band IIR filters.

II. Perfect-Reconstruction Two-Channel IIR Filter Banks. These banks are generated by using both causal and anti-causal half-band IIR filters.

Two-Channel IIR Filter Banks with Phase Distortion

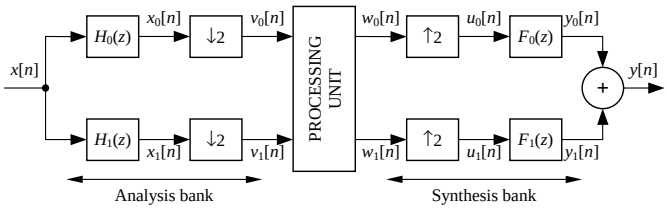

Figure 1. Two-channel filter bank.

- The above figure shows again a two-channel filter bank consisting of analysis and synthesis parts as well as the processing unit.
- It is again assumed that the processing unit causes no distortion, that is, $w_0[n] \equiv v_0[n]$ and $w_1[n] \equiv v_1[n]$.
- We recall that the relation between the z-transforms of the input and output signals of Figure 1 is given by

$$Y(z) = T(z)X(z) + A(z)X(-z), \tag{1a}$$

where

$$T(z) = \frac{1}{2}\left[H_0(z)F_0(z) + H_1(z)F_1(z)\right] \tag{1b}$$

and

$$A(z) = \frac{1}{2}\left[H_0(-z)F_0(z) + H_1(-z)F_1(z)\right]. \tag{1c}$$

- We select $H_0(z)$ and $H_1(z)$ to be a power-complementary lowpass–highpass half-band IIR filter pair.
- In this case (see Part II.G: Half-Band IIR Filters, Pages 246-266 in Part II, for details),

$$H_0(z) = (1/2)\left[A_0(z^2) + z^{-1}A_1(z^2)\right] \tag{2a}$$

and

$$H_0(z) = (1/2)\left[A_0(z^2) + z^{-1}A_1(z^2)\right] \tag{2b}$$

with

$$A_0(z) = \prod_{k=1}^{K_0} \frac{a_k^{(0)} + z^{-1}}{1 + a_k^{(0)} z^{-1}} \tag{2c}$$

and

$$A_1(z) = \prod_{k=1}^{K_1} \frac{a_k^{(1)} + z^{-1}}{1 + a_k^{(1)} z^{-1}} \tag{2d}$$

being allpass filters of orders K_0 and K_1, respectively.

- The overall filter order is $2(K_0 + K_1) + 1$ and it is required that $K_0 = K_1$ or $K_0 = K_1 + 1$.
- Selecting

$$F_0(z) = 2H_1(-z) = 2H_0(z) = A_0(z^2) - z^{-1}A_1(z^2) \tag{3a}$$

and

$$F_1(z) = -2H_0(-z) = -2H_1(z) = -A_0(z^2) + z^{-1}A_1(z^2) \tag{3b}$$

Equation (1) takes the following form:

$$Y(z) = T(z)X(z), \tag{4a}$$

where

$$T(z) = z^{-1}A_0(z^2)A_1(z^2). \tag{4b}$$

- Since $A_0(z^2)$ and $A_1(z^2)$ are allpass filters, the overall frequency response is expressible, after some manipulations, as

$$T(e^{j\omega}) = e^{j\phi(\omega)}, \tag{5a}$$

where

$$\phi(\omega) = -(2K_0 + 2K_1 + 1)\omega - \sum_{k=1}^{K_0} 2\tan^{-1}\left(\frac{-a_k^{(0)}\sin(2\omega)}{1 + a_k^{(0)}\sin(2\omega)}\right) - \sum_{k=1}^{K_1} 2\tan^{-1}\left(\frac{-a_k^{(1)}\sin(2\omega)}{1 + a_k^{(1)}\sin(2\omega)}\right). \tag{5b}$$

- Hence, the amplitude response is identically equal to zero and the input-output relation suffers only from a phase distortion.
- This distortion is tolerable in audio applications provided that the distortion is not too large.
- Figure 2 shows implementations for the overall system.
- The second one using the commutative models is the most efficient one.

- The third implementation is obtained assuming the outputs of the processing unit are identical to the inputs and it is removed.
- Then, by rearranging the terms, we arrive at this structure.
- In this structure, the input-output relation is redrawn in a form corresponding to the input-output relation as given by Equation (4).

Figure 2. Efficient Implementations for a Two-Channel Filter Bank Based on the Use of Conventional Causal Half-Band IIR Filters.

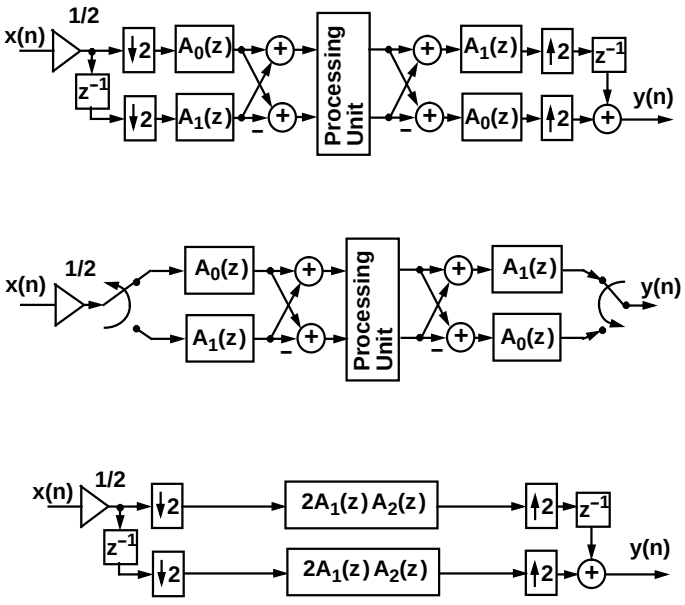

Example: $\omega_s = 0.586\pi$ and the Minimum Stopband Attenuation is at least 80 dB

- Here, the stopband edge is selected to be $\omega_s = 0.586\pi$ in order to make the comparison of the resulting bank with earlier two-channel FIR filter bank designs possible.
- The given criteria are met by

$$A_0(z) = \prod_{k=1}^{3} \frac{a_k^{(0)} + z^{-1}}{1 + a_k^{(0)} z^{-1}}$$

and

$$A_1(z) = \prod_{k=1}^{2} \frac{a_k^{(1)} + z^{-1}}{1 + a_k^{(1)} z^{-1}},$$

where $a_1^{(0)} = 0.059868$, $a_2^{(0)} = 0.424962$, $a_3^{(0)} = 0.874343$, $a_1^{(1)} = 0.217298$, and $a_2^{(1)} = 0.645857$.

- This is a special lowpass–highpass elliptic filter pair of order 11 designed by a routine written by Renfors and Saramäki.
- The following three pages illustrate the characteristics of the resulting overall two-channel IIR filter bank.
- It should be pointed out that the approximately linear-phase half-band filters are not considered here. The main reason is that they also cause some phase distortion for the overall transfer function especially in the transition band region.

Amplitude responses for the analysis and synthesis filters in an example two-channel IIR filter bank

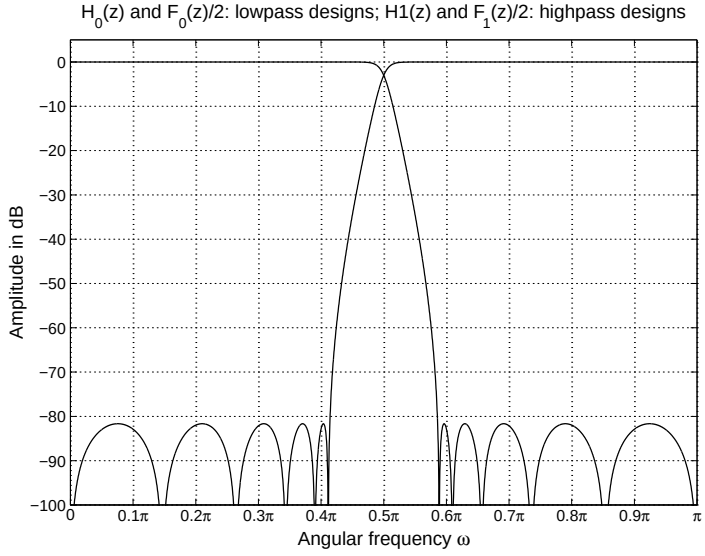

Pole-zero plots for the analysis and synthesis filters in an example two-channel IIR filter bank

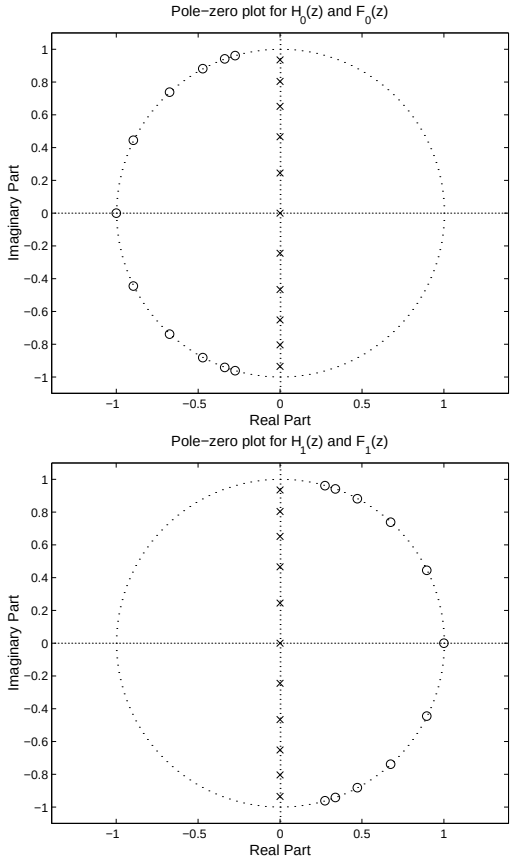

Responses for the input-output transfer function of an example two-channel IIR filter bank

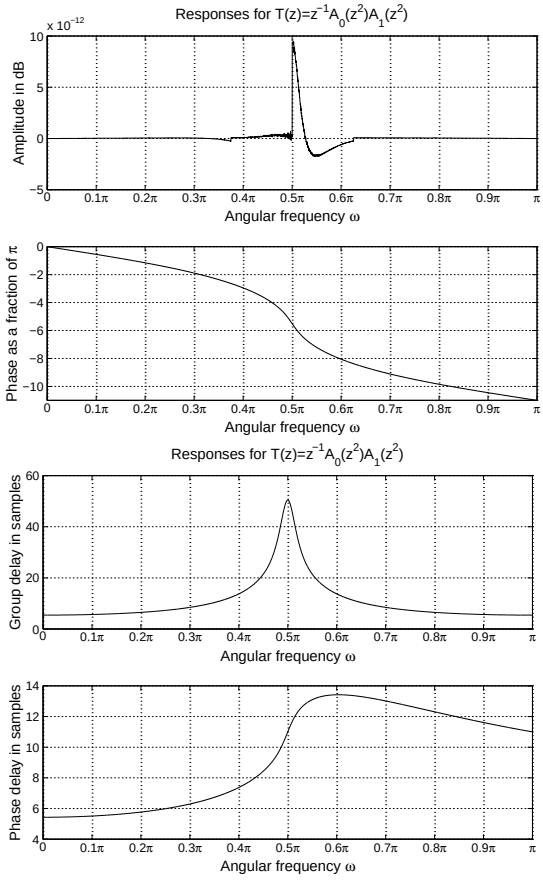

Two-Channel IIR Filter Banks without Phase Distortion

- We select

$$H_0(z) = (1/2)\left[A_0(z^2) + z^{-1}A_1(z^2)\right], \quad (6a)$$

$$H_1(z) = H_0(-z) = (1/2)\left[A_0(z^2) - z^{-1}A_1(z^2)\right], \quad (6b)$$

$$F_0(z) = 2H_0(z^{-1}) = A_0(z^{-2}) + zA_1(z^{-2}), \quad (6c)$$

and

$$F_1(z) = 2H_1(z^{-1}) = A_0(z^{-2}) - zA_1(z^{-2}). \quad (6d)$$

- Substituting these into Equation (1) yields

$$Y(z) \equiv X(z). \quad (7)$$

- Looks ideal! Figure 3 shows implementations for the overall filter bank. The first one is the actual implementation and the second one is an equivalent structure (not used for implementation purposes).
- The main problem in the proposed implementation is that both $F_0(z)$ and $F_1(z)$ are anti-causal filters.
- For finite length signals (like images), there are several ways of implementing the filter bank using the corresponding causal filters. Implementations are also possible for infinite length signals.

.

- The explanation of these implementation forms is out the scope of these lecture notes. If you interested in these forms, contact the lecturer.
- It should be pointed out that in these implementations, there is a need to produce a time-reversed version of the input data before and after filtering.
- This introduces an extra delay. Delay-free systems cannot be implemented!

Figure 3. Implementations for a Two-Channel Filter Bank Based on the Use of Causal and Anti-Causal Half-Band IIR Filters.

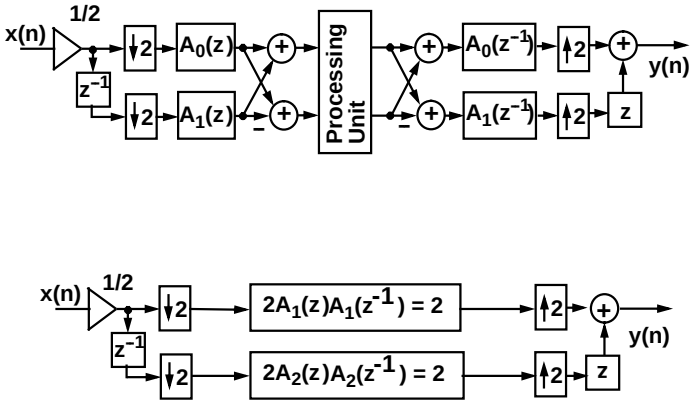

Part V.C: Tree-Structured Filter Banks

- When generating a tree-structured filter bank, we start with a two-channel filter bank as shown in Figure 1(a). For this bank, the analysis and synthesis filters are denoted by $H_0^{(1)}(z)$, $H_1^{(1)}(z)$, $F_0^{(1)}(z)$, and $F_1^{(1)}(z)$.
- The next step is to remove the processing unit in Figure 1(a) and produce $y_0^{(1)}(n)$ $[y_1^{(1)}(n)]$ from $x_0^{(1)}(n)$ $[x_1^{(1)}(n)]$ using a two-channel filter bank as shown in Figure 1(b). For this bank, the analysis and synthesis filters are denoted by $H_0^{(2)}(z)$, $H_1^{(2)}(z)$, $F_0^{(2)}(z)$, and $F_1^{(2)}(z)$.
- This gives a two-level tree-structured filter bank shown in Figure 1(c).
- The three-level tree-structured filter bank shown in Figure 2 is obtained by removing the processing unit in Figure 1(c) and producing $y_k^{(2)}(n)$ from $x_k^{(2)}(n)$ for $k = 0,1,2,3$ using a two-channel filter bank with the analysis and synthesis filters being $H_0^{(3)}(z)$, $H_1^{(3)}(z)$, $F_0^{(3)}(z)$, and $F_1^{(3)}(z)$.

Figure 1. Generation of a Two-Level Tree-Structured Filter Bank.

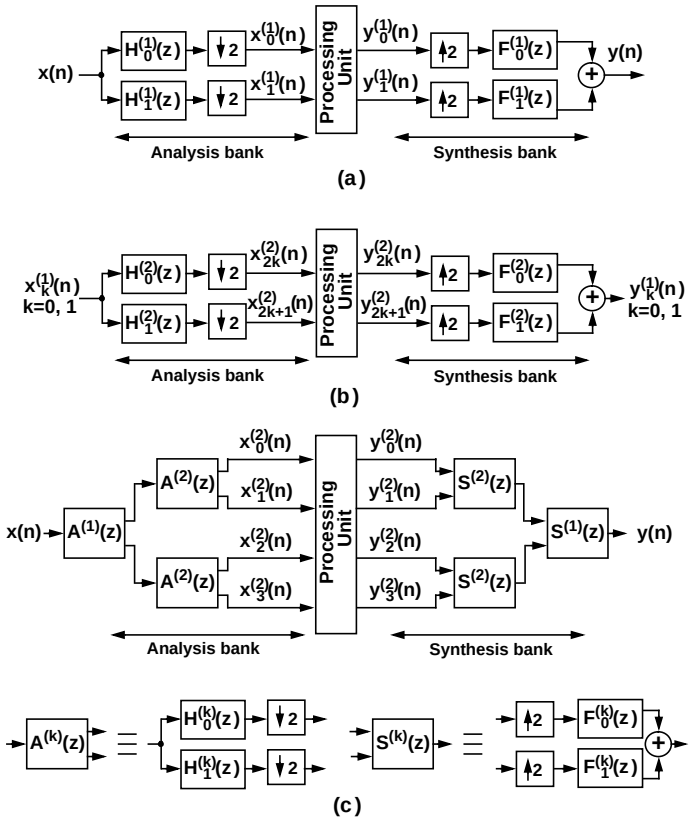

Figure 2. Three-Level Tree-Structured Filter Bank.

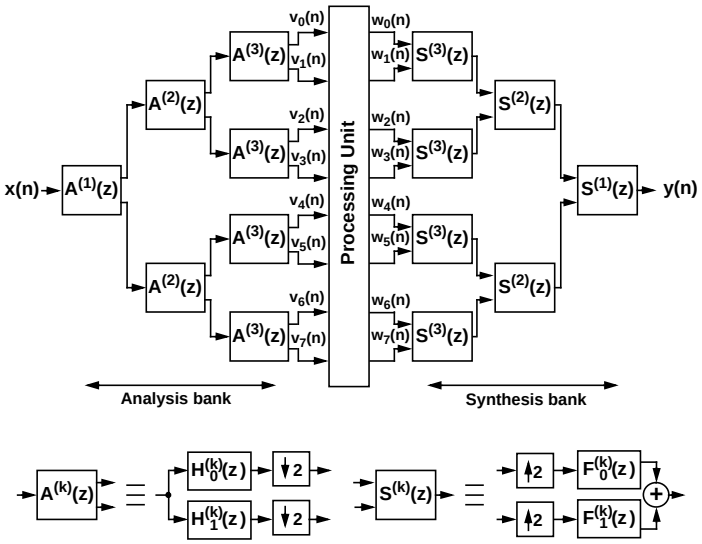

Analysis of the Performance of the Tree-Structured Filter Bank

- In order to analyze the performance of the three-level tree-structure filter bank of Figure 2, it is redrawn into the equivalent form shown in Figure 3.
- Hence, it corresponds to an analysis-synthesis bank with 8 channels.
- A four-level bank can be generated by removing the processing unit and producing $w_k^{(3)}(n)$ from $v_k^{(3)}(n)$ for $k = 0,1,\cdots,7$ using a two-channel filter bank with the analysis and synthesis filters being $H_0^{(4)}(z)$, $H_1^{(4)}(z)$, $F_0^{(4)}(z)$, and $F_1^{(4)}(z)$.
- In this case, the number of channels is 16.
- In general for a *M*-level tree-structured filter bank, the number of channels is 2^M.
- Next an example will be given illustrating how to select the building-block two-channel filter banks.

Figure 3. Equivalent Structure for the Three-Level Tree-Structured Filter Bank of Figure 2.

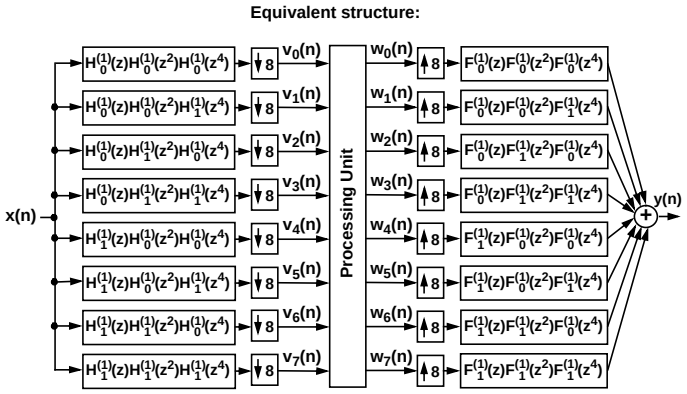

Example

- It is desired to generate an analysis-synthesis filter bank with 8 channels by using a three-level tree-structured filter bank.
- The required transition bandwidth and the attenuation are 0.05π and 60 dB, respectively.
- This bank is constructed by using the following analysis and synthesis filters for $k = 1, 2, 3$:

$$H_0^{(k)}(z) = (1/2)\left[A_0^{(k)}\left(z^2\right) + z^{-1}A_1^{(k)}\left(z^2\right)\right], \qquad (1a)$$

$$H_1^{(k)}(z) = (1/2)\left[A_0^{(k)}\left(z^2\right) + z^{-1}A_1^{(k)}\left(z^2\right)\right], \qquad (1b)$$

$$F_0^{(k)}(z) = A_0^{(k)}\left(z^2\right) - z^{-1}A_1^{(k)}\left(z^2\right), \qquad (1c)$$

and

$$F_1^{(k)}(z) = -A_0^{(k)}\left(z^2\right) + z^{-1}A_1^{(k)}\left(z^2\right) \qquad (1d)$$

with

$$A_0^{(k)}(z) = \prod_{l=1}^{K_0^{(k)}} \frac{a_{k,l}^{(0)} + z^{-1}}{1 + a_{k,l}^{(0)} z^{-1}} \qquad (1e)$$

and

$$A_1^{(k)}(z) = \prod_{l=1}^{K_1^{(k)}} \frac{a_{k,l}^{(1)} + z^{-1}}{1 + a_{k,l}^{(1)} z^{-1}}\,. \qquad (1f)$$

- Hence, IIR two-channel filter banks considered in Part V.B are used.
- The desired overall performance is achieved by designing the first, second, and third two-channel filter bank in such a way that the stopband edges for the lowpass analysis filter are located at $\omega_s = 0.525\pi$, $\omega_s = 0.55\pi$, and $\omega_s = 0.6\pi$, respectively.
- Note that for the first filter, the transition bandwidth is the specified one.
- For the second and third ones, they are two and four times the specified one, respectively.
- For all the building-block two-channel filter banks, the required attenuation is the specified one, that is, 60 dB.
- For the first filter bank, $K_0^{(1)} = K_1^{(1)} = 3$, $a_{1,1}^{(0)} = 0.086411$, $a_{1,2}^{(0)} = 0.522945$, $a_{1,3}^{(1)} = 0.849610$, $a_{1,1}^{(1)} = 0.293592$, $a_{1,2}^{(1)} = 0.711961$, and $a_{1,3}^{(1)} = 0.952906$.
- For the second filter bank, $K_0^{(2)} = 3$, $K_1^{(2)} = 2$, $a_{2,1}^{(0)} = 0.082947$, $a_{2,2}^{(0)} = 0.519644$, $a_{2,3}^{(1)} = 0.910331$, $a_{2,1}^{(1)} = 0.285641$, $a_{2,2}^{(1)} = 0.729135$.
- For the third filter bank, $K_0^{(3)} = K_1^{(3)} = 2$, $a_{3,1}^{(0)} = 0.079866$, $a_{3,2}^{(0)} = 0.545324$, $a_{3,1}^{(1)} = 0.28382$, and $a_{3,2}^{(1)} = 0.834411$.

- Figures 4 and 5 show the responses for the analysis and synthesis filters in the three building-block two-channel IIR filter banks.
- Figure 6 shows the amplitude responses between the input $x(n)$ and $v_k(n)$ for $k = 0,1,\cdots,7$ (see Figures 2 and 3). The numbers in the figure indicate the corresponding response.
- The responses between $w_k(n)$ for $k = 0,1,\cdots,7$ and the output $y(n)$ are the same with the exception that they are multiplied by eight.
- Figure 7 shows how the fifth bank can be generated according to the equivalent structure of Figure 3.
- The input-output tranfer function is given by

$$T(z) = z^{-7} A_0^{(1)}(z^2) A_1^{(1)}(z^2) A_0^{(2)}(z^4) A_1^{(2)}(z^4) A_0^{(3)}(z^8) A_1^{(3)}(z^8). \quad (2)$$

- Figure 8 shows various responses for this transfer function.

Figure 4. Amplitude responses for the analysis and synthesis filters in the first and second building blocks.

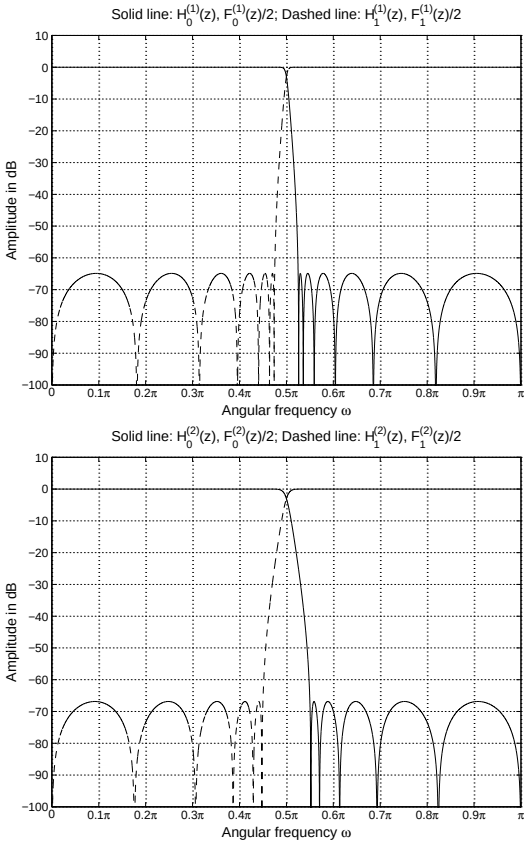

Figure 5. Amplitude responses for the analysis and synthesis filters in the third building block.

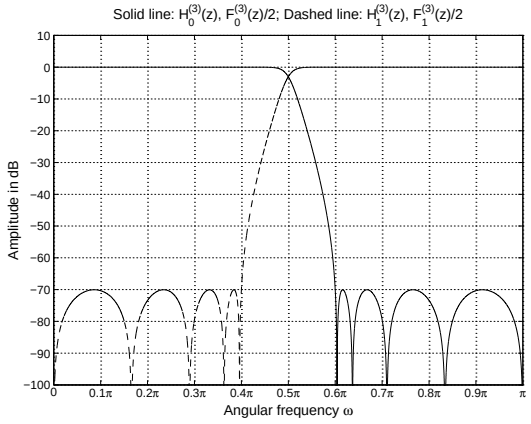

Figure 6. Amplitude responses for the resulting filters between the input $x(n)$ and $v_k(n)$ for $k = 0,1,\cdots,7$. The numbers in the figure indicate the corresponding responses.

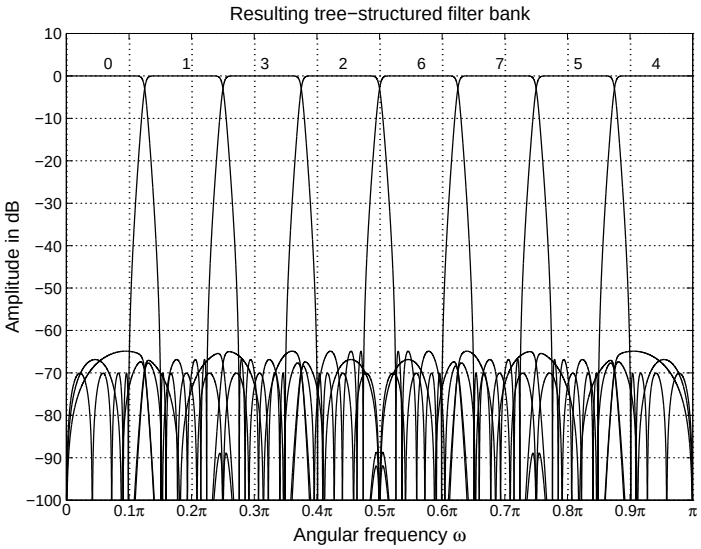

Figure 7. Generation of the fifth bank according to the equivalent structure of Figure 3.

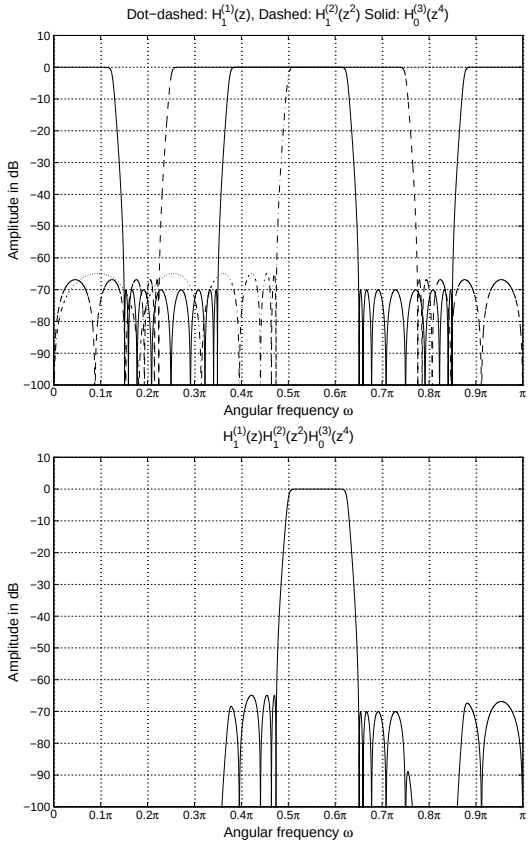

Figure 8. Responses for the input-output transfer function of an example tree-structured IIR filter bank

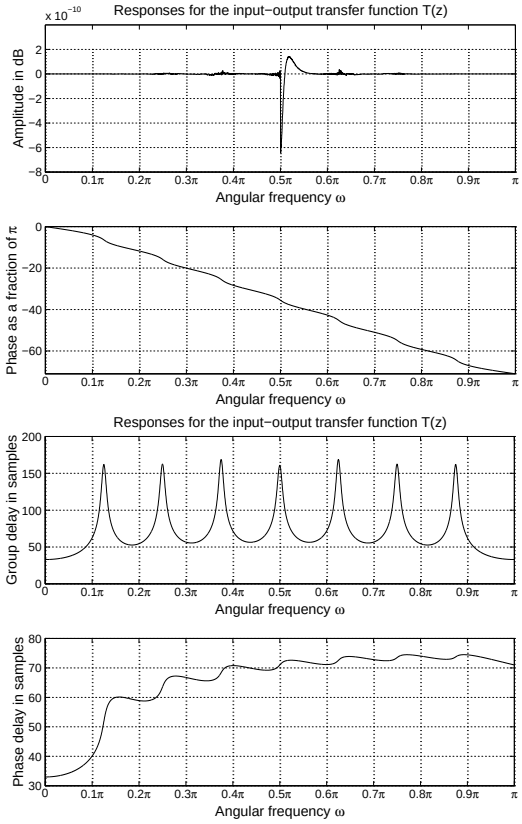

Part V.C: Discrete-Time Wavelet Banks

- The theory behind wavelets is very mathematical and complicated especially in the case of continuous-time wavelets.
- This part shows what are discrete-time wavelet banks and how to generate them easily from special two-channel filter banks.
- The filter bank approach for explaining the wavelet theory is for engineers easier to understand and makes the theory very compact.
- In the end of this pile, some connections to continuous-time wavelets are shown.
- Therefore, we proceed in the opposite manner: mathematicians start with continuous-time wavelets and use them for generating discrete-time wavelet banks
- We start with the discrete-time wavelet banks and show how to generate continuous-time wavelets based on the use of multilevel wavelet banks.
- We are not considering in details the applications. It would be a topic of another course!
- Hopefully, this part helps the reader to somehow understand the wavelet theory especially when applied to processing discrete-time signals. After reading this pile, the reader is encouraged to look at the MATLAB Wavelet Toolbox manual. Good luck!

Organization of This Pile of Lecture Notes

- We concentrate on the following topics:

I. Generation of wavelet banks based on the use of several copies of the same two-channel filter bank

II. Orthogonal (paraunitary) FIR wavelet banks derived from maximally-flat half-band FIR filters

III. Biorthogonal FIR wavelet banks derived from maximally-flat half-band FIR filters

IV. Generalized orthogonal FIR wavelet banks

V. Generalized biorthogonal FIR wavelet banks

VI. How to measure the "goodness" of wavelet banks

VII. Comments